



저작자표시-비영리-변경금지 2.0 대한민국

이용자는 아래의 조건을 따르는 경우에 한하여 자유롭게

- 이 저작물을 복제, 배포, 전송, 전시, 공연 및 방송할 수 있습니다.

다음과 같은 조건을 따라야 합니다:



저작자표시. 귀하는 원저작자를 표시하여야 합니다.



비영리. 귀하는 이 저작물을 영리 목적으로 이용할 수 없습니다.



변경금지. 귀하는 이 저작물을 개작, 변형 또는 가공할 수 없습니다.

- 귀하는, 이 저작물의 재이용이나 배포의 경우, 이 저작물에 적용된 이용허락조건을 명확하게 나타내어야 합니다.
- 저작권자로부터 별도의 허가를 받으면 이러한 조건들은 적용되지 않습니다.

저작권법에 따른 이용자의 권리는 위의 내용에 의하여 영향을 받지 않습니다.

이것은 [이용허락규약\(Legal Code\)](#)을 이해하기 쉽게 요약한 것입니다.

[Disclaimer](#)

이학박사학위논문

**Development of  
Thermo-Responsive Materials  
and Their Potential Application  
of Osmotic Control**

온도응답성 물질의 개발 및 삼투조절로의 응용

2016년 2월

서울대학교 대학원

화학부 생화학전공

노 민 우

# Development of Thermo-Responsive Materials and Their Potential Application of Osmotic Control

지도교수 이 연

이 논문을 이학박사학위논문으로 제출함

2016년 2월

서울대학교 대학원

화학부 생화학전공

노 민 우

노민우의 박사학위논문을 인준함

2016년 2월

위 원 장	<u>박 종 상</u>	(인)
부 위 원 장	<u>이 연</u>	(인)
위 원	<u>손 병 혁</u>	(인)
위 원	<u>정 택 동</u>	(인)
위 원	<u>서 지 훈</u>	(인)

## Abstract

“Smart materials” response to not only the physical signals such as temperature, light, and magnetic field but also chemical signals such as ionic concentration, glutathione concentration, and pH, etc. Among them temperature has some advantages. Temperature could be easily applied to biosystem by heat pad or near-infrared illumination. It can be also cooled or heated reversibly.

Thermoresponsive materials which consist of two or more components change physical or chemical properties by mild temperature changes. Among them I have more interested in water-soluble thermoresponsive materials. The water is not only present in a large amount enough to covers approximately 71% of the earth surface but also forming the body fluids of all living organisms on the earth. Therefore, water-soluble thermoresponsive materials could be applicable for biomedical application as well as water purification. In practice, these materials have been extensively researched in various applications such as cell culture dishes, chromatography, temperature-triggered drug release, or targeted drug delivery.

Thermoresponsive materials in aqueous solution could be classified into two and the phase transition behavior in water could be explained by simplified thermodynamic equation.

$$\Delta G_m = \Delta H_m - T\Delta S_m$$

(The Gibbs free energy of mixing:  $\Delta G_m$ , The enthalpy of mixing:  $\Delta H_m$ , The entropy of mixing:  $\Delta S_m$ , Temperature; T)

Materials that can mix in solvent below a certain temperature and abruptly phase separate from solution above a certain temperature are referred as the lower critical solution temperature (LCST). Representative LCST materials are poly(N-isopropylacrylamid

e) of which structure harmoniously consist of hydrophilic moiety and hydrophobic moiety. In aqueous solutions of these polymers,  $\Delta H_m$  is negative due to strong interaction between water and polymer molecules and  $\Delta S_m$  is also negative because the hydrophobic moieties (isopropyl) of poly(N-isopropylacrylamide) are captured in ordered form of water molecules which actually existed in disordered form. Therefore, at a given composition and pressure, LCST phase separation occurs when  $\Delta G_m$  becomes zero as the negative  $T\Delta S_m$  becomes dominant over the negative  $\Delta H_m$  upon reaching a specific temperature.

On the contrary to LCST phase transition, materials which are miscible in solvent above a certain temperature and abruptly phase separate from solution below a certain temperature are referred as the upper critical solution temperature (UCST). Representative UCST materials are poly(3-dimethyl(methacryloyloxyethyl) ammonium propane sulfonate) which has both positively charged ammonium moiety and negatively charged sulfonate in every repeating unit, which can strongly interact with each other by electrostatic interaction generating positive value of  $\Delta H_m$ . Therefore, UCST phase separation occurs when temperature reaches below a certain temperature to give rise to zero value of  $\Delta G_m$  as the positive  $\Delta H_m$  becomes dominant over the positive  $T\Delta S_m$  upon reaching a specific temperature.

In order to synthesize the thermoresponsive materials previously, monomer should be synthesized and then polymerized through multiple steps. I have been focusing on researches for synthesizing water-soluble thermoresponsive materials in a simple way comparing to conventional methods in this work. In order to achieve above goal I purchased the commercially available amine rich pol

ymer, branched polyethylenimine (*b*-PEI) which can be easily modified through simple reaction such as acylation, ring opening reaction, or methylation for synthesizing LCST materials or UCST materials.

LCST properties were introduced into *b*-PEI by simple acylation. The resulting *N*-acylated *b*-PEI have similar structure with poly(*N*-isopropylacrylamide). The phase transition temperature of *N*-acylated *b*-PEI in aqueous solution can be controlled by the hydrophobicity of acyl group, degree of acylation, concentration, and pH in the range of 10–90 °C

UCST properties were introduced into *b*-PEI by ring-opening reaction resulting in *N*-sulfopropylated *b*-PEI which has similar structure with poly(3-dimethyl(methacryloyloxyethyl) ammonium propane sulfonate). The phase transition temperature of *N*-sulfopropylated *b*-PEI in aqueous solution can be controlled by degree of acylation, molecular weight, concentration, and pH in the range of 10–90 °C

Another way to introduce the UCST properties into *b*-PEI is to simply mix with hydrogen halide or by methylation of *b*-PEI. Although halide salts of *b*-PEI exhibited the UCST properties in water, the pH of solution is too low to apply for practical application. However, methylated *b*-PEI (MPEI) derivatives which possess 35–38% quaternary ammoniums with hydrophobic counter anions such as iodide ( $I^-$ ) or tetrafluoroborate ( $BF_4^-$ ) exhibited UCST in mild pH range because of strong electrostatic interaction and hydrophobic interaction. Methylated *b*-PEI with more hydrophilic anion such as  $Cl^-$  and  $Br^-$  did not show UCST properties because the hydrophobicity of anions is not enough to have strong interaction with MPEI. The dependence of salt effect and molecular weight

ht on phase transition temperature is also investigated.

The new application such as a draw solute for forward osmosis (FO) is possible thanks to easy introduction of thermoresponsiveness into amine-rich polymer by above methods. The FO method is to draw fresh water from feed solution to a draw solution (Higher concentration than feed solution) by spontaneous osmosis through a semipermeable membrane. Following the Van't Hoff equation,

$$\pi = c.R.T = w/(V.M).R.T$$

( $\pi$ : osmotic pressure,  $c$ : molarity of concentration,  $R$ : gas constant,  $T$ : temperature,  $V$ : volume,  $M$ , molecular weight,  $w$ : solute weight)

thermoresponsive materials with low molecular weight are needed for inducing high osmotic pressure. Therefore, *n*Bu-TAEA with low molecular weight, 356g/mol, was synthesized, which exhibited 20–30 °C phase transition temperature at 2.2 M in water. After phase separation at 55 °C, the effective osmotic pressure of *n*Bu-TAEA solution became lower than 0.15 M equivalent to physiological saline. Therefore, after fresh water could be drawn from 0.60 M NaCl solution equivalent to seawater, to 2.2 M of *n*Bu-TAEA solution below phase transition temperature, the obtained fresh water in *n*Bu-TAEA solution was released into 0.15 M equivalent to physiological saline above phase transition temperature. The thermoresponsive materials as a draw solute for forward osmosis could be energy efficient method for obtaining fresh water from seawater.

Keywords

Thermoresponsive materials, Lower critical solution temperature (LCST), Upper critical solution temperature (UCST), Forward osmo

sis (FO), Branched polyethylenimine (*b*-PEI)

Student number : 2010-20275



## Contents

Contents.....	i
List of figures.....	v
List of tables.....	ix
.	
Part I. Novel lower critical solution temperature phase transition materials effectively control osmosis by mild temperature changes	
1. Abstract.....	1
2. Introduction.....	2
3. Materials and Methods.....	5
3.1. Materials.....	5
3.2. Synthesis of acylated TAEA.....	5
3.3. Characterization of thermosensitive solutes.....	6
3.4. Analysis of osmotic flow.....	6
4. Results and Discussion.....	8
4.1. Synthesis and solubility of acyl-TAEA.....	8
4.2. LCST transition behavior of acyl-TAEA in water.....	8
4.3. Temperature-dependent osmotic flux of <i>n</i> Bu-TAEA.....	9
4.4. Possibility as draw solutes for a forward osmosis (FO).....	11

5. Conclusions.....	13
6. References.....	14

Part II. Introduction of pH-sensitive upper critical solution temperature (UCST) properties into branched polyethylenimine

1. Abstract.....	25
2. Introduction.....	26
3. Materials and Methods.....	30
3.1. Materials.....	30
3.2. Synthesis of <i>N</i> -sulfopropylated polyethylenimine.....	30
3.3. Measurement of UCST phase transition.....	31
3.4. Titration of <i>N</i> -sulfopropylated polyethylenimine.....	31
3.5. Cytotoxicity assay.....	32
4. Results and Discussion.....	33
4.1. Synthesis of <i>N</i> -sulfopropylated-polyethylenimine.....	33
4.2. Phase transition behavior of <i>N</i> -sulfopropylated-polyethylenimine in water.....	34
4.3. Ionic strength-UCST relationship of <i>N</i> -sulfopropylated-polyethylenimineI.....	37
4.4. pH-UCST relationship of <i>N</i> -sulfopropylated-polyethylenimine.....	38
4.5. Cytotoxicity assay.....	40
5. Conclusions.....	42
6. References.....	43

Part III. Upper critical solution temperature (UCST) phase transition of halide salts of branched polyethylenimine and methylated branched polyethylenimine in aqueous solutions

1. Abstract.....	56
2. Introduction.....	58
3. Materials and Methods.....	60
3.1. Materials.....	60
3.2. Synthesis of methylated polyethylenimine halide.....	60
3.3. Measurement of the UCST phase transition.....	61
4. Results and Discussion.....	62
4.1. Phase transition behavior of various polyethylenimine halide salts.....	62
4.2. Preparation of methylated polyethylenimine halide.....	63
4.3. Phase transition behavior of methylated PEI halide.....	64
4.4. Effect of counter ions in methylated polyethylenimine backbone.....	65
5. Conclusions.....	68
6. References.....	69

## List of figures

### Part I. Novel lower critical solution temperature phase transition materials effectively control osmosis by mild temperature changes

- Figure 1.** Schematic diagram of thermosensitive control of osmosis and structures of thermosensitive acyl-TAEA derivatives.....16
- Figure 2.** (a) LCST transition of acyl-TAEA derivatives. The phase transition of Val-TAEA was measured for the water : ethanol (10 : 1) cosolvent. (b) Phase diagram of *n*Bu-TAEA - water mixture.....17
- Figure 3.** (a) Simplified structure of temperature-controlled osmosis system. (b) The control of osmosis at 16 °C and (c) at 55 °C. (d) Osmotic flux from NaCl solution to *n*Bu-TAEA solution at 21 °C. (e) Reversed osmotic flux from *n*Bu-TAEA solution to NaCl solution at 55 °C. (f) Reproducibility of temperature-based control of osmotic flow. Numbers (1 - 3) represent the heating and cooling cycle. F and R represent the osmotic flows at 21 °C and 55 °C, respectively.....18
- Figure 4.** <sup>1</sup>H-NMR spectra of (a) *n*Bu-TAEA, (b) *i*Bu-TAEA, (c) Val-TAEA in D<sub>2</sub>O.....19
- Figure 5.** (a) Concentration-phase transition temperature relationship of *n*Bu-TAEA (The molarity was calculated on the basis of the density at 25 °C). (b) Molecular weight-phase transition temperature relationship of thermosensitive solutes. The phase transition was measured at the same mass concentration of 70 g/L.....20
- Figure 6.** Reproducibility of the phase transition of *n*Bu-TAEA at the concentration of 1.5 M.....21
- Figure 7.** Titration profile *n*Bu-TAEA at the concentration of 0.1 M...22

## Part II. Introduction of pH-sensitive upper critical solution temperature (UCST) properties into branched polyethylenimine

<b>Figure 1.</b> Synthetic scheme of <i>N</i> -sulfopropylated <i>b</i> -PEI.....	46
<b>Figure 2.</b> <sup>1</sup> H NMR spectrum of PS <sub>0.59</sub> -PEI (1800) in D <sub>2</sub> O (0.97 %wt NaOD).....	47
<b>Figure 3.</b> Phase diagram of (A) PS <sub>0.59</sub> -PEI(1800), (B) PS <sub>0.80</sub> -PEI(1800), and (C) PS <sub>0.82</sub> -PEI(600) in water. (D) UCST transition of 5 %wt PS <sub>0.59</sub> -PEI(1800).....	48
<b>Figure 4.</b> Effect of ionic strength on the phase transition temperature of (A) PS <sub>0.59</sub> -PEI(1800) (7.0 %wt; pH 7.0) and (B) PS <sub>0.80</sub> -PEI(1800) (10 %wt; pH 2.8).....	49
<b>Figure 5.</b> Effect of pH on the phase transition temperature of (A) PS <sub>0.59</sub> -PEI(1800) (7.0 %wt; 90 mM NaCl) and (B) PS <sub>0.46</sub> -PEI (1800) (5.0 %wt; 122 mM NaCl).....	50
<b>Figure 6.</b> Comparison of buffering capacity of <i>b</i> -PEI(1800), PS <sub>0.46</sub> -PEI(1800), PS <sub>0.59</sub> -PEI(1800), and PS <sub>0.80</sub> -PEI(1800) at varying pH values.....	51
<b>Figure 7.</b> The proposed mechanism of the pH-dependent UCST phase separation of PS-PEI derivatives.....	52
<b>Figure 8.</b> Relative viability of HeLa cells treated with PS-PEI derivatives. Each data point represents the average value of four experiments (±S.D.).....	53
<b>Figure 9.</b> <sup>1</sup> H NMR spectra of PS <sub>0.46</sub> -PEI(1800) (A), PS <sub>0.80</sub> -PEI(1800) (B), PS <sub>0.60</sub> -PEI(600) (C), and PS <sub>0.82</sub> -PEI(600) (D) in D <sub>2</sub> O (0.97 wt% NaOD).....	54

**Figure 10.**  $^{13}\text{C}$  NMR INVGATE spectra of PS<sub>0.46</sub>-PEI(1800) (A), PS<sub>0.59</sub>-PEI(1800) (B), PS<sub>0.80</sub>-PEI(1800) (C), PS<sub>0.60</sub>-PEI(600) (D), and PS<sub>0.82</sub>-PEI(600) (F) in D<sub>2</sub>O (0.97 wt% NaOD).....55

### Part III. Upper critical solution temperature (UCST) phase transition of halide salts of branched polyethylenimine and methylated branched polyethylenimine in aqueous solutions

**Figure 1.** (A) Interaction between ammonium residues and halide counterions in PEI halide salts. (B) Phase transition of PEIB at 30 % (w/w) polymer composition at various ratios of HBr/N ratio (C) Phase transition of PEIB at various compositions, HBr/N ratio of 1.5.....72

**Figure 2.** (A) Preparation of various methylated PEI (MPEI) salts by methylation and anion exchange. (B) Phase transition of MPEII<sub>0.35</sub> (25 kDa) (C) Composition - temperature phase diagram of MPEII<sub>0.38</sub> (0.80 kDa).....73

**Figure 3.** (A) Change of phase transition temperature of MPEI<sub>0.35</sub> (25 kDa) at various counter-ion composition and the total anion concentration. (B) Composition - temperature phase diagram of MPEI(BF<sub>4</sub>)<sub>0.35</sub> (25 kDa).....74

**Figure 4.** (A) Phase transition behavior of PEIB at HBr/N ratio or 2. (B) Phase transition behavior of PEIB at HBr/N ratio or 2.5 . (C) Phase transition behavior of PEII at a polymer composition of 35 % (w/w) and HI/N ratio of 1.5. (D) Phase transition behavior of PEIC at a polymer composition of 20 % (w/w) and HCl/N ratio of 4.0.....75

**Figure 5.** The inverted gate (INVGATE) <sup>13</sup>C NMR spectra of MPEII<sub>0.35</sub> (25 kDa) (A) and MPEII<sub>0.38</sub> (0.80 kDa) (B).....76

**Figure 6.** Hysteresis of MPEII<sub>0.35</sub> (25 kDa) at 20 % (w/w) polymer composition.....77



## List of tables

### Part I. Novel lower critical solution temperature phase transition materials effectively control osmosis by mild temperature changes

**Table 1.** Solubility and phase transition temperature of *N*-acyl TAEA derivatives.....23

**Table 2.** Permeation/rejection percentage of NaCl and *n*Bu-TAEA through the semipermeable membrane.....24

### Part II. Introduction of pH-sensitive upper critical solution temperature (UCST) properties into branched polyethylenimine

**Table 1.** Synthesized PS-PEI derivatives.....56

### Part III. Upper critical solution temperature (UCST) phase transition of halide salts of branched polyethylenimine and methylated branched polyethylenimine in aqueous solutions

**Table 1.** pH values of (A) the PEI halide solutions and (B) MPEII solutions.....78

List of publication.....	79
Abstract in Korean (국문초록).....	81

## Part I. Novel lower critical solution temperature phase transition materials effectively control osmosis by mild temperature changes

### 1. Abstract

Osmosis can be controlled reversibly and effectively by mild temperature changes based on novel thermosensitive solutes with LCST transition. The *n*Bu-TAEA thermosensitive solution can draw fresh water from seawater at temperatures less than the phase separation temperature, and the osmotic flow was reversed at higher temperatures.

## 2. Introduction

Osmosis is a promising potential means for the efficient production of energy and resources. So-called 'blue energy,' which is generated by the salt concentration gradient between river and seawaters, represents several terawatts on a global scale.<sup>1</sup> Meanwhile, more than 40,000,000 m<sup>3</sup> of seawater are desalinated against the salt gradient worldwide every day due to increasing demands for fresh water.<sup>2</sup> If the direction of the concentration gradient could be controlled by mild temperature changes that may be achieved easily by waste heat or sunlight irradiation, it would facilitate the utilization of osmotic power as an energy source as well as more efficient and practical desalination. Here I show the temperature-sensitive control of osmosis using solute materials with reversible lower critical solution temperature (LCST) transitions.

Some thermosensitive solutes exhibit phase separation from one-phase solution when heated over a certain temperature, referred to as the lower critical solution temperature (LCST) transition.<sup>3</sup> Since the concentration of the solution is dramatically decreased after phase separation, the LCST transition can also be applied to the temperature-sensitive control of concentration gradients. The reversibility as well as the rapidity of the LCST transition make the utilization of the thermosensitive solutes very attractive. Moreover, thermosensitive solutes with transition temperatures ranging from 20 °C to 30 °C can be synthesized by a delicate design of the molecular structure. This feasible temperature range can allow for less overall energy input into the system to induce transition. I have focused on the

development of solute materials with LCST characteristics for the reversible control of osmosis within a practical temperature range.

The osmotic pressure of a solution can be calculated by the van't Hoff equation:

$$\Pi = iRTc$$

where  $i$  is the van't Hoff factor,  $R$  is the gas constant,  $T$  is the temperature, and  $c$  is the molarity of the solution. The concentration of seawater is equivalent to 0.60 M of NaCl at 25 °C.

If I produce a thermosensitive solution with a higher concentration than 1.2 M, assuming that  $i$  of the thermosensitive solute is 1, osmotic flow can be induced from the seawater to the thermosensitive solution at a temperature lower than its transition temperature (Fig. 1). In contrast, at temperatures higher than the transition temperature, the effective molarity of the solution sharply decreases due to the aggregation of thermosensitive solute molecules, and the direction of osmotic flow can be reversed. Therefore, not only is high molar solubility of the thermosensitive solute required for effective water drawing, but large  $\Delta c$  against the temperature change is also required for the effective control of osmotic flow by temperature changes.

I selected  $N,N',N''$ -triacylated tris(2-aminoethyl)amine (acyl-TAEA) derivatives as thermosensitive solutes with low transition temperature, high molar solubility, and large  $\Delta c$ .  $N$ -Acylated polyethylenimine derivatives have structural similarities to well-known thermosensitive polymers,<sup>4</sup> poly( $N$ -acylacrylamide)

and poly(*N*-alkyloxazoline), which exhibit LCST transitions ranging from 10 °C to 90 °C depending on the hydrophobicity of their acyl groups as given in a previous report.<sup>5</sup> However, thermosensitive non-polymer solutes with low molecular weight are required to produce high molarity solutions because molecular weight is inversely proportional to molarity. Therefore, I examined the thermosensitivity of acyl-TAEA derivatives because their structures are similar to the core structures of *N*-acylated polyethylenimine derivatives.

### 3. Materials and Methods

#### 3.1. Materials

Tris(2-aminoethyl)amine (TAEA), butyric anhydride, isobutyric anhydride, and valeroyl chloride were purchased from Aldrich (USA). Sodium hydroxide (NaOH), sodium bicarbonate (NaHCO<sub>3</sub>), magnesium sulfate (MgSO<sub>4</sub>), methanol, methylene chloride, and pyridine were purchased from Daejung (Korea). Cellulose trifluoroacetate was purchased from Hydration Technology Innovation (HTI, USA). All reagents were used without further purification.

#### 3.2. Synthesis of acylated TAEA derivatives

Thermosensitive solutes were synthesized by a previously described method with some modifications.<sup>8</sup> Tris(2-aminoethyl)amine (TAEA) (10.0 mL; 64.0 mmol) was dissolved in 400 mL of 1M NaHCO<sub>3</sub> in methanol. Butyric anhydride and isobutyric anhydride were slowly added to the solution at 0 °C with vigorous stirring. After 1 h stirring at 0 °C, the solution was further stirred for 18 h at ambient temperature. The pH of the reaction mixture was adjusted to about 11 with 1M NaOH, and the mixture was extracted with methylene chloride (×3). The organic extracts were dried with MgSO<sub>4</sub>, and evaporated under vacuum to produce the final product, acylated TAEA as a white solid. Val-TAEA was synthesized from valeroyl chloride and TAEA in methylene chloride solvent with pyridine by a similar method as described above. The <sup>1</sup>H-NMR

spectra of acylated TAEA derivatives are shown in Figure 4.

### 3.3. Characterization of thermosensitive solutes

The LCST phase transitions of solutions containing thermosensitive solutes were measured by a UV-Vis spectrophotometer. By increasing the temperature, the transmittance at a wavelength of 600 nm was measured to determine the phase transition temperature. The phase transition temperature was defined at which the transmittance was below 5 %.

### 3.4. Analysis of osmotic flow

The osmotic flow was measured using a handmade U-shaped glass tube. A semipermeable membrane (diameter: 3.3 cm) made from cellulose trifluoroacetate was placed in the middle of the tube and each tube was filled with *n*Bu-TAEA solutions or NaCl solutions, respectively. The selective layer of the semipermeable membrane was faced toward the *n*Bu-TAEA solutions. The temperature was controlled by thermostat water bath. Osmotic water flux from NaCl solutions to *n*Bu-TAEA solutions was calculated from the volumetric change of each solution during 1 h after 1 h-stabilization at 21 ( $\pm 2$ ) °C. (In the case of 1.8 M and 2.2 M *n*Bu-TAEA, the flux at 18 ( $\pm 2$ ) °C was measured instead.) The reversal of osmotic flow was similarly calculated using the volumetric change at 55 ( $\pm 2$ ) °C.

The remaining *n*Bu-TAEA concentrations in the H<sub>2</sub>O-rich phase after phase separation were measured using HPLC. The



penetration of NaCl and solute molecules through the semipermeable membrane was determined by using an inductively coupled plasma emission spectrometer and HPLC, respectively. The permeation percentage of solute  $A$  ( $\%P_A$ ) was calculated by an equation:

$$\%P_A = \frac{C_A' \times V}{C_A \times v} \times 100$$

where  $C_A$  is the initial concentration of  $A$  solution,  $v$  is the volume of permeated water,  $C_A'$  is the concentration of  $A$  on the other side of the membrane after the osmosis, and  $V$  is the volume of the solution of the other side of the membrane. The permeation percentage is shown in Table 2.

## 4. Results and Discussion

### 4.1. Synthesis and solubility of acyl-TAEA

Acyl-TAEA derivatives can be synthesized by a reaction between TAEA and acylating agents. *n*-Butyryl, isobutyryl, and valeroyl groups were introduced into the TAEA core to produce *n*Bu-TAEA, *i*Bu-TAEA, and Val-TAEA, respectively. Given that the hydrophobicity of an acyl group increases as the carbon number increases, the aqueous solubility generally decreases as the carbon number increases (Table 1). The molarities of solutions were calculated based on the density at 25 °C for comparisons of the concentrations. Although Val-TAEA presents solubility problems in water, *i*Bu-TAEA can be dissolved up to a concentration of 0.28 M and *n*Bu-TAEA was found to be miscible over the concentration of 2.2 M, which is much higher than the ionic concentration of seawater.

### 4.2. LCST transition behavior of acyl-TAEA in water

The LCST transition of the aqueous solution of acyl-TAEA was examined according to the transmittance change (Fig. 2).<sup>6</sup> The transition temperature of acyl-TAEA is inversely related to solubility. As the hydrophobicity of the acyl group is increased, the entropy of mixing between acyl-TAEA and water ( $\Delta S_{\text{mix}}$ ) becomes more negative, so that phase separation occurs at a lower temperature at which the Gibbs free energy of mixing ( $\Delta G_{\text{mix}} = \Delta H_{\text{mix}} - T\Delta S_{\text{mix}}$ ) becomes positive.<sup>4</sup> At the same concentration of 0.20 M, *n*Bu-TAEA and *i*Bu-TAEA exhibited

phase separation at 54 °C and 39 °C, respectively (Fig. 2a). The more hydrophobic Val-TAEA presented the lowest transition temperature of 17 °C at a concentration of 0.074 M in a water : ethanol (10 : 1) mixture.

As shown in the phase diagram of *n*Bu-TAEA (Fig. 2b), lower transition temperatures were generally observed at higher concentrations. As the concentration increased from 0.20 M to 2.1 M, the phase transition temperature decreased from 54 °C to 20 °C. Acyl-TAEA, however, exhibited phase separation from water at higher temperatures compared to its polymeric correspondent, *N*-acylated polyethylenimine, mainly due to the conformational entropic factor ( $\Delta S_{\text{con}}$ ) of the thermosensitive dissolution (Fig. 5b).  $\Delta S_{\text{mix}}$  can be expressed as the sum of the conformational entropy ( $\Delta S_{\text{con}}$ ), which reflects positional combinations of solvent and solute molecules, and the interaction entropy ( $\Delta S_{\text{int}}$ ), which originates from the solvent - solute interaction.<sup>7</sup> Since the  $\Delta S_{\text{con}}$  of a polymer solute is less positive than the  $\Delta S_{\text{con}}$  of a low-molecular-weight solute, the resulting  $\Delta S_{\text{mix}}$  of *N*-acylated polyethylenimine is more negative than the  $\Delta S_{\text{mix}}$  of acyl-TAEA.

### 4.3. Temperature-dependent osmotic flux of *n*Bu-TAEA

On the basis of these results, I chose *n*Bu-TAEA as a thermosensitive solute with both a practical transition temperature and high aqueous solubility. I attempted to confirm temperature controlled osmosis between NaCl solutions and the thermosensitive solution containing *n*Bu-TAEA (Fig. 3a). First, I evaluated the drawing activity of the *n*Bu-TAEA solution from NaCl solutions at a temperature lower than the phase transition

temperature (Fig. 3b and d). The osmotic flux through a semipermeable cellulose trifluoroacetate membrane was expressed as litres per square metre per hour ( $\text{L m}^{-2} \text{h}^{-1}$ ; LMH). Higher flux was induced as the concentration gradient between two solutions increased. I observed that 0.50 M *n*Bu-TAEA solution (mole fraction of *n*Bu-TAEA ( $X_{n\text{Bu-TAEA}}$ ) = 0.011) exhibited 0.25 LMH against physiological saline (0.15M NaCl), but presented a LMH over 0.91 against 0.050 M NaCl solution. Although 1.0 M ( $X_{n\text{Bu-TAEA}}$  = 0.027) and 2.0 M *n*Bu-TAEA solutions ( $X_{n\text{Bu-TAEA}}$  = 0.096) showed higher osmotic flux than 0.50 M *n*Bu-TAEA, they did not draw water from 0.60 M NaCl solution (equivalent to seawater). When 2.2 M *n*Bu-TAEA solution ( $X_{n\text{Bu-TAEA}}$  = 0.11) was used, the osmotic flow from 0.60 M NaCl solution was attained. The effective drawing of *n*Bu-TAEA from the seawater equivalent is an encouraging result, because solutions containing other low-molecular-weight thermosensitive materials such as triethylamine (TEA) or glycol ether cannot effectively draw water from seawater equivalent (data not shown).<sup>8</sup>

Osmotic flow was clearly reversed at a temperature higher than the phase transition temperature (Fig. 3c and e). The osmotic flux of 0.1 - 0.8 LMH was induced from the phase-separated *n*Bu-TAEA suspension to the NaCl solution. The reversed osmotic flow was mainly dependent upon the concentration of the NaCl solution. At all three compositions ( $X_{n\text{Bu-TAEA}}$  = 0.022, 0.038, 0.066), similar osmotic flux values were observed against the same NaCl solution. The remaining *n*Bu-TAEA concentrations in the H<sub>2</sub>O-rich phase after phase separation were measured to be about 0.20 M for all three compositions. Therefore, similar osmotic flux values were induced by similar concentration

gradients. The abrupt decrease in the effective concentrations from 1.6 M to 0.20 M during the phase separation can induce osmotic flow from *n*Bu-TAEA solution to even physiological saline (0.15 M NaCl).

The temperature-sensitive control of osmosis between 0.50 M NaCl solution and 1.8 M *n*Bu-TAEA solution can be visualized using a U-tube. The volume of the *n*Bu-TAEA solution was increased, whereas the volume of the NaCl solution was decreased at 16 - 20 °C. On the other hand, reversed flow was detected by heating to 53 - 57 °C. The reversal of the osmotic flow by temperature control is not a one-off phenomenon. As expected from the reproducibility or repetitiveness of the phase transition of 1.5 M *n*Bu-TAEA solution (Fig. 6), the osmotic flux at both temperatures was maintained almost constantly over three cycles of heating and cooling (Fig. 3f). The direction of osmotic flow can be controlled effectively and reproducibly by the LCST transition of a thermosensitive solute according to simple and mild changes in temperature.

#### **4.4. Possibility as draw solutes for a forward osmosis (FO)**

A forward osmosis (FO) technique uses the concentration gradient between seawater and draw solutions with higher concentrations for desalination.<sup>9</sup> The draw solution, with its higher concentration, can attract fresh water from seawater and then release freshwater by a separation process. Theoretically, net energy is required only in the separation and recycling of draw solutes so that the energy efficiency of FO is far better than reverse osmosis (RO).<sup>10</sup> A pilot scale FO plant based on

draw solutes of ammonium carbonate is now in operation, but the potential damage to the FO membrane due to the very high pH values of the draw solution and the relatively difficult recycling process are obstacles to overcome. Several draw solutes have been tested to replace ammonium carbonate but most still have difficulty in drawing fresh water from high salt feed solutions such as seawater.<sup>11</sup> *n*Bu-TAEA, a low-molecular-weight LCST molecule, can be soluble in water up to a high molar concentration which enables the drawing of fresh water from a seawater equivalent at low temperature and release of the drawn water by mild heating. Moreover, the *n*Bu-TAEA solution is only weakly basic, with a pH value of 8.1 at the concentration of 1.5 M, so that damage to membrane walls might be much less severe when compared to ammonium carbonate solutions. The pKa value of *n*Bu-TAEA was measured as 5.9 (Fig. 7), which is significantly lower than that of other tertiary amines such as triethylamine (pKa = 10.7). The electro-withdrawing effect of three amide moieties and the steric factor can lower the pKa value of *n*Bu-TAEA effectively.

## 5. Conclusions

I demonstrated the control of osmotic flow between the ranges of 18 °C and 55 °C. Considering that phase transition temperature can be precisely controlled by the structural design of a thermosensitive solute, the control of osmosis is also possible at biologically tolerable temperature ranges. In addition, the development of lower-molecular-weight thermosensitive solutes with lower diffusion constants (Table 1) can help the increase of osmotic flux into practical ranges because the osmotic flux is closely related to internal concentration polarization of solutes in the membrane layer.<sup>12</sup> Along with the development of more selective and efficient semipermeable membranes than commercially available membranes,<sup>13</sup> this concept of simple and effective thermosensitive osmotic control can be applied to a variety of scientific and engineering fields using concentration gradients.

## 6. References

1. P. van Helden, *EMBO Rep.*, 2011, 12, 2; P. Ball, *Nat. Mater.*, 2011, 10, 344.
2. Q. Schiermeier, *Nature*, 2008, 452, 260; M. Elimelech and W. A. Phillip, *Science*, 2011, 333, 712.
3. R. B. Griffiths and J. C. Wheeler, *Phys. Rev. A*, 1970, 2, 1047.
4. H. G. Schild, *Prog. Polym. Sci.*, 1992, 17, 163; J.-S. Park, Y. Akiyama, F. M. Winnik and K. Kataoka, *Macromolecules*, 2004, 37, 6786.
5. H. Kim, S. Lee, M. Noh, S. H. Lee, Y. Mok, G. Jin, J.-H. Seo and Y. Lee, *Polymer*, 2011, 52, 1367.
6. Y. Haba, A. Harada, T. Takagishi and K. Kono, *J. Am. Chem. Soc.*, 2004, 126, 12760.
7. Y. Gnanou and M. Fontanille, *Organic and physical chemistry of polymers*, WILEY-Interscience, 2008, ch. 4.
8. A. Ikehata, C. Hashimoto, Y. Mikami and Y. Ozaki, *Chem. Phys. Lett.*, 2004, 393, 403; S. P. Christensen, F. A. Donate, T. C. Frank, R. J. LaTulip and L. C. Wilson, *J. Chem. Eng. Data*, 2005, 50, 869.
9. R. L. McGinnis and M. Elimelech, *Environ. Sci. Technol.*, 2008, 42, 8625; L. A. Hoover, W. A. Phillip, A. Tiraferri, N. Y. Yip and M. Elimelech, *Environ. Sci. Technol.*, 2011, 45, 9824.
10. J. R. McCutcheon, R. L. McGinnis and M. Elimelech, *Desalination*, 2005, 174, 1; R. L. McGinnis and M. Elimelech, *Desalination*, 2007, 207, 370.
11. M. M. Ling, K. Y. Wang and T.-S. Chung, *Ind. Eng. Chem. Res.*, 2010, 49, 5869; M. M. Ling, T.-S. Chung and X. Lu, *Chem. Commun.*, 2011, 47, 10788 - 10790; D. Li, X. Zhang, J. Yao, G. P.



Simon and H. Wang, Chem. Commun., 2011, 47, 1710.

12. J. R. McCutcheon and M. Elimelech, AIChE J., 2007, 53, 1736.

13. X. Song, Z. Liu and D. D. Sun, Adv. Mater., 2011, 23, 3256; A.

Noya, H. G. Park, F. Fornasiero, J. K. Holt, C. P. Grigoropoulos  
and O. Bakajin, Nano Today, 2007, 2, 22.

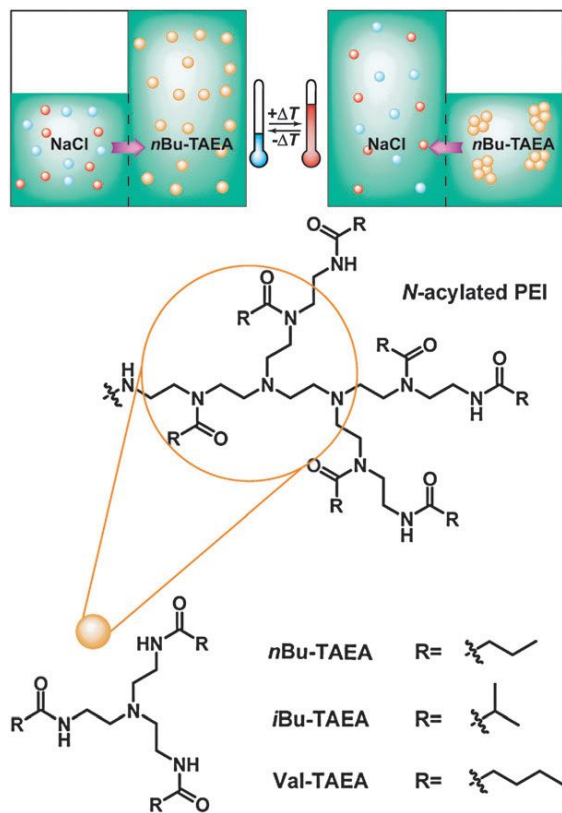


**Figure 1.** Schematic diagram of thermosensitive control of osmosis and structures of thermosensitive acyl-TAEA derivatives.

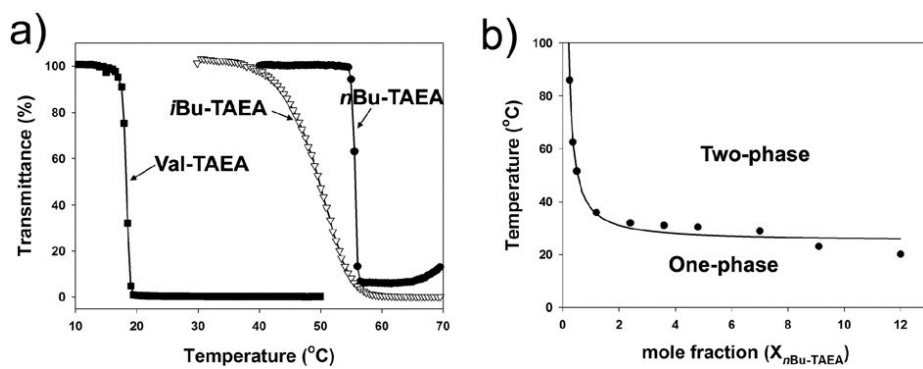


**Figure 2.** (a) LCST transition of acyl-TAEA derivatives. The phase transition of Val-TAEA was measured for the water : ethanol (10 : 1) cosolvent. (b) Phase diagram of *n*Bu-TAEA - water mixture.

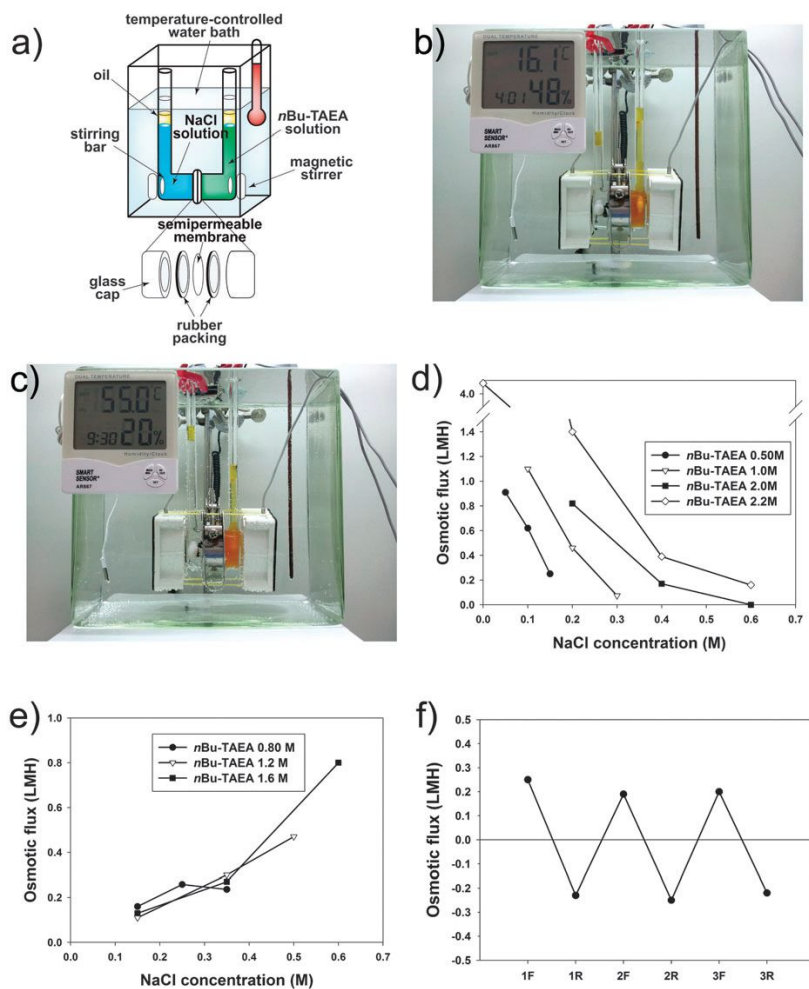


**Figure 3.** (a) Simplified structure of temperature-controlled osmosis system. (b) The control of osmosis at 16 °C and (c) at 55 °C. (d) Osmotic flux from NaCl solution to *n*Bu-TAEA solution at 21 °C. (e) Reversed osmotic flux from *n*Bu-TAEA solution to NaCl solution at 55 °C. (f) Reproducibility of temperature-based control of osmotic flow. Numbers (1 - 3) represent the heating and cooling cycle. F and R represent the osmotic flows at 21 °C and 55 °C, respectively.

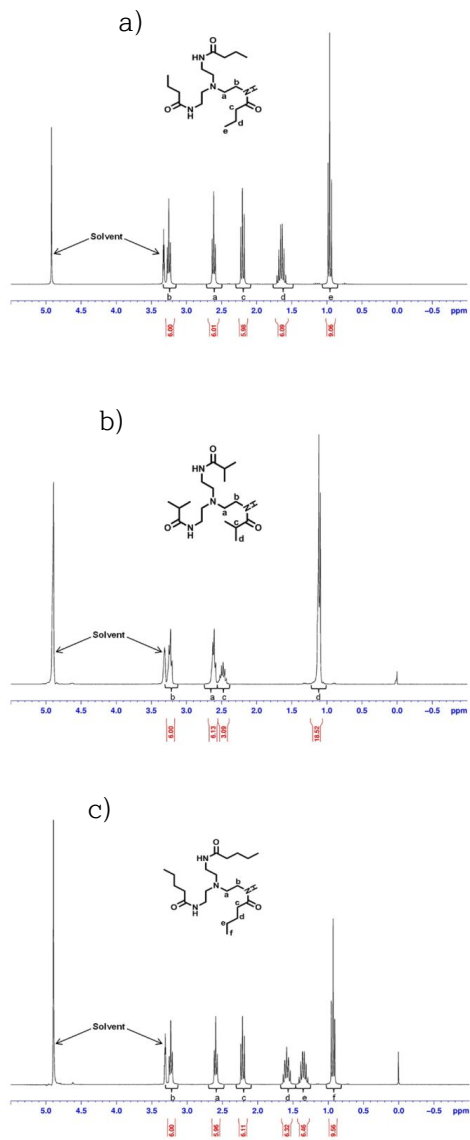


**Figure 4.**  $^1\text{H}$ -NMR spectra of (a) *n*Bu-TAEA, (b) *i*Bu-TAEA, (c) Val-TAEA in  $\text{D}_2\text{O}$ .

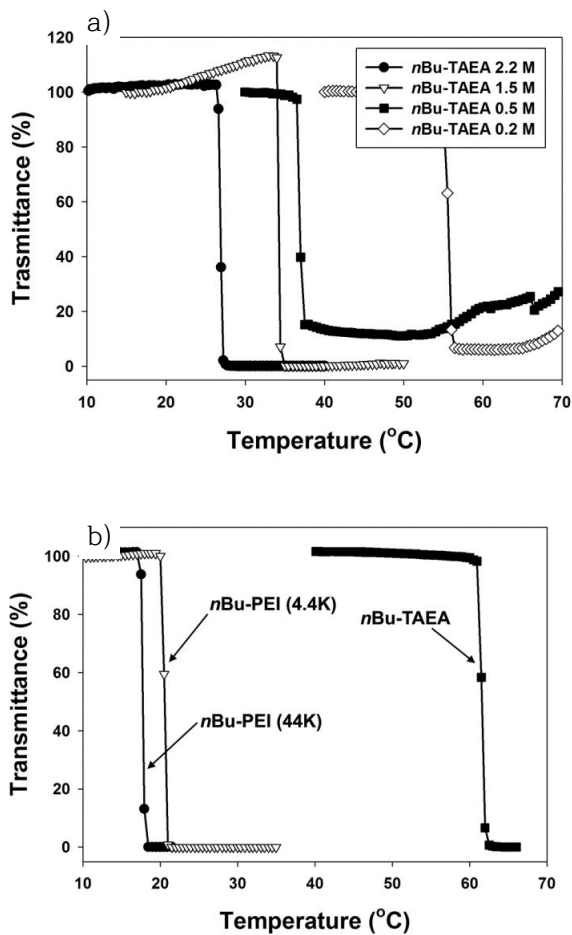


**Figure 5.** (a) Concentration-phase transition temperature relationship of *n*Bu-TAEA (The molarity was calculated on the basis of the density at 25 °C). (b) Molecular weight-phase transition temperature relationship of thermosensitive solutes. The phase transition was measured at the same mass concentration of 70 g/L.

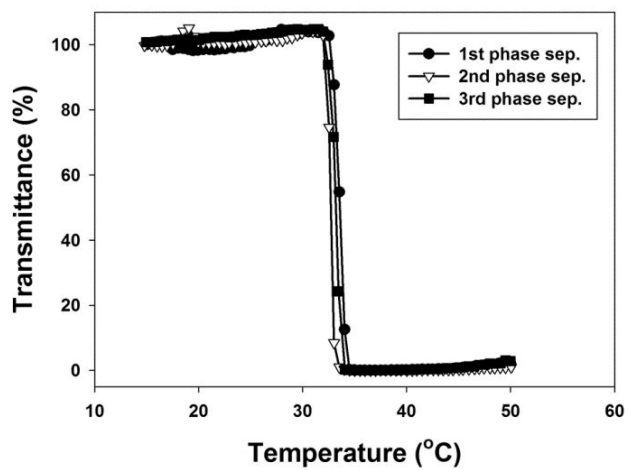


**Figure 6.** Reproducibility of the phase transition of *n*Bu-TAEA at the concentration of 1.5 M.

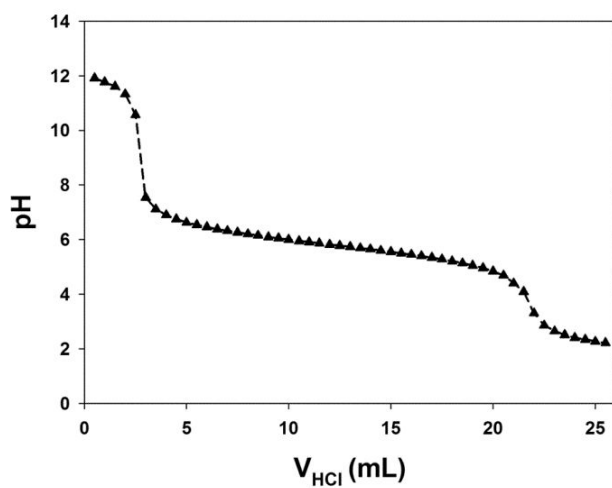


**Figure 7.** Titration profile *n*Bu-TAEA at the concentration of 0.1 M.



**Table 1.** Solubility and phase transition temperature of *N*-acyl TAEA derivatives.

N-acyl TAEA derivatives	Molecular weight	Diffusion coefficient ( $D/10^{-9} \text{ m}^2\text{s}^{-1}$ ) <sup>a</sup>	Solubility (mol/L) <sup>b</sup>	Phase transition temperature (°C) <sup>c</sup>	
				at 0.20M	at the max. concentration
<i>n</i> Bu-TAEA	356.5	0.29	2.2	54	23
<i>i</i> Bu-TAEA	356.5	0.31	0.28	39	33
Val-TAEA	398.6	0.26	0.074 <sup>d</sup>	-	17

<sup>a</sup>The diffusion coefficient was calculated by using Stokes–Einstein equation assuming that *N*-acyl derivatives have spherical shape.

<sup>b</sup>The molarity was calculated on the basis of the density at 25°C.

<sup>c</sup>The phase transition temperature is corresponding to 1.0 % decrease of the transmittance at 600 nm.

<sup>d</sup>The solubility of Val-TAEA was measured in the water : ethanol (10 : 1) co-solvent.

**Table 2.** Permeation/rejection percentage of NaCl and *n*Bu-TAEA through the semipermeable membrane.

Permeated solute	Initial concentration (mol/L) <sup>a</sup>	Transferred concentration (mol/L) <sup>a</sup>	Permeation [rejection] (%)
NaCl	0.30	0.0048 <sup>b</sup>	1.6 [98.4]
<i>n</i> Bu-TAEA	1.5	0.024 ( $\pm 0.0035$ ) <sup>c</sup>	1.6 [98.4] ( $\pm 0.22$ )

<sup>a</sup>The molarity was calculated on the basis of the density at 25 °C.

<sup>b</sup>The NaCl concentration was measured by inductively coupled plasma emission spectrometer.

<sup>c</sup>The concentration of *n*Bu-TAEA was measured by HPLC.

## Part II. Introduction of pH-sensitive upper critical solution temperature (UCST) properties into branched polyethylenimine

### 1. Abstract

I introduced upper critical solution temperature (UCST) properties into an amine-rich polymer, branched polyethylenimine (*b*-PEI) by a simple sulfopropylation reaction. The phase transition behavior of the *N*-sulfopropylated *b*-PEI (PS-PEI) derivatives was influenced by the degree of sulfopropylation, concentration, molecular weight, ionic strength, and pH. In particular, the phase transition temperature of PS-PEI was strongly dependent upon pH. As the pH decreased, the protonable amine residues of PS-PEI became positively charged and interacted strongly with the negatively charged sulfonate residues, exhibiting the increase of the UCST phase transition temperature.

## 2. Introduction

Polyethylenimine (PEI) has been widely used as a chelating agent, detergent, and adhesive in various fields, including water purification<sup>1</sup>, cosmetic industries<sup>2</sup>, and paper industries<sup>3</sup>. The various applications of PEI are related to the PEI backbone, which can effectively chelate metal ions and interact with various types of chemical residues through electrostatic interactions, coordinate bonds, or hydrogen bonds. In particular, the biomedical applications of PEI are closely related with the pH-dependent protonation of the amine residues. The amine residues in the PEI backbone are partially protonated at a neutral pH, and the positively charged PEI can form a complex with negatively charged plasmid DNA<sup>4</sup>, antisense DNA<sup>5</sup>, or small interfering RNA (siRNA)<sup>6</sup> by electrostatic interactions. The PEI-genetic materials complex can be internalized by cells via endocytic processes, and the delivered genetic materials can exhibit their biomedical activity in the cytosol or nucleus. Since PEI was first used as a gene delivery carrier<sup>7</sup>, it has been recognized as a gold standard among nonviral gene delivery carriers due to its high delivery efficiency<sup>8</sup>.

As safety and specificity have become important concerns in biomedical applications, various methods for a more precise control of the activity of biomaterials have been developed. So-called 'smart' control or 'signal-responsive' control of bioactivity is now highlighted in the development of biomaterials [9]. Physical signals such as light<sup>10</sup>, ultrasound<sup>11</sup>, and temperature change<sup>12</sup> or chemical signals such as ionic strength<sup>13</sup>, glutathione

concentration<sup>14</sup>, pH<sup>15</sup>, and enzymes<sup>16</sup> are considered to be controlling switches for smart biomaterials. Among these switches, temperature change is readily available in the biosystem because it can be induced internally by inflammation or excessive metabolism in tissues, and it can also be generated externally by a heat pad<sup>17</sup> or near-infrared illumination<sup>18</sup>.

The potential of PEI as a biomaterial, as well as the usefulness of the temperature signal, inspired us to introduce temperature sensitivity to the amine-rich PEI backbone. Although temperature sensitivity can be defined using various terms, lower critical solution temperature (LCST) transition<sup>19</sup> (phase separation above a certain temperature) and upper critical solution temperature (UCST) transition<sup>20</sup> (phase separation below a certain temperature) are often used to describe temperature-sensitive materials in biomedical applications. Previously, I successfully introduced LCST properties into branched PEI (*b*-PEI) by a simple acylation procedure<sup>21</sup>. The acylated *b*-PEI is miscible with aqueous solutions below the phase transition temperature (10–90 °C), and it precipitates above the phase transition temperature, which is influenced by the degree of acylation, ionic strength, and pH.

In the current study, our aim was to introduce UCST properties into *b*-PEI by a simple sulfopropylation reaction (Fig. 1). It was reported that linear PEI (*l*-PEI) showed a UCST-type phase transition<sup>22</sup>, but the phase transition temperature is too high (64 °C) to be applied into biosystem. And there has been no report about the control of UCST phase transition temperature of *b*-PEI or *l*-PEI. Although reports about UCST polymers in aqueous

solutions are rather limited compared to LCST polymers<sup>23</sup>, some polymers with quaternary ammonium-sulfonate zwitterionic pairs, such as poly-3-dimethyl(methacryloyloxyethyl) ammonium propane sulfonate<sup>24</sup> and poly(3-[*N*-(3-methacrylamidopropyl)-*N,N*-dimethyl])ammonio propane sulfonate<sup>25</sup>, exhibited a UCST-type phase transition in aqueous solutions. The strong electrostatic interaction between the positive quaternary ammonium residue and the negative sulfonate residue significantly enhances the enthalpy of mixing ( $\Delta H_m$ ), and the UCST phase transition occurs at the temperature (*T*) where the Gibbs free energy of mixing ( $\Delta G_m = \Delta H_m - T\Delta S_m$ ) changes from positive to negative values<sup>26</sup>. Because primary, secondary, and tertiary amines in the *b*-PEI backbone can react with 1,3-propanesultone (PS) via nucleophilic ring opening, I could obtain *N*-sulfopropylated *b*PEI polymers with several amine/ammonium-sulfonate pairs without the preparation of zwitterionic monomers.

Although tertiary amines produce quaternary ammoniums by a reaction with PS, primary and secondary amines produce secondary and tertiary amines, respectively. The pH-sensitivity, which is an important characteristic of *b*-PEI for biomaterials, can be maintained by the remaining protonable amine residues. In addition, because the remaining amines can be protonated into ammoniums under acidic conditions, which can also interact with sulfonate residues via electrostatic interaction, it was hypothesized that the UCST behavior of *N*-sulfopropylated *b*-PEI would be strongly dependent upon the degree of protonation. In this paper, the UCST properties of the newly synthesized *N*-sulfopropylated *b*-PEI polymers were carefully examined with

varying degrees of *N*-sulfopropylation, molecular weights, ionic strength, and pH for future applications of *N*-sulfopropylated *b*-PEI polymers, as well as the development of other UCST polymers from pre-existing polymers based on this simple sulfopropylation method.

### 3. Materials and Methods

#### 3.1. Materials

Two branched polyethylenimine (*b*-PEI) polymers ( $M_n = 600$ , PD ( $M_w/M_n$ ) = 1.3, and  $M_n = 1800$ , PD ( $M_w/M_n$ ) = 1.1), 1,3-propanesultone, and 3-(4,5-dimethyl-2-thiazolyl)-2,5-diphenyl-2H-tetrazolium bromide (MTT) were purchased from Aldrich (USA). Methanol and sodium hydroxide (NaOH) were purchased from Daejung (Korea). Dulbecco's modified Eagle's medium (DMEM), Dulbecco's phosphate buffered saline (DPBS) and fetal bovine serum (FBS) were purchased from WelGENE (USA). All reagents were used without further purification.

#### 3.2. Synthesis of *N*-sulfopropylated polyethylenimine

A solution of *b*-PEI in methanol (10.0% w/v) was slowly added to an energetically stirred solution of 1,3-propanesultone in methanol (30 mL) at 45 °C. The feed ratios between 1,3-propanesultone and reactive amines in *b*-PEI are summarized in Table 1. After 24 h stirring, a pale yellow precipitate was collected from the mixture by filtration. The precipitate was re-dissolved in 2 M NaOH aqueous solution (10 mL). The solution was dialyzed against deionized water four times using a dialysis membrane (Spectrum Laboratories, Inc. (USA); MWCO = 1000) to remove NaOH and low-molecular weight impurities. The



dialyzed solution was lyophilized to prepare the product as a pale yellow powder.  $^1\text{H}$  NMR (Agilent 400-MR DD2 (400 MHz)) spectra of *N*-sulfopropylated polyethylenimine are shown in Fig. 2 and Fig. 9. The degree of *N*-sulfopropylation and the relative compositions of protonable amines and unprotonable quaternary ammoniums, which were calculated from the  $^1\text{H}$  NMR and  $^{13}\text{C}$  NMR spectra, are summarized in Table 1.

### 3.3. Measurement of UCST phase transition

The UCST phase transition of aqueous *N*-sulfopropylated polyethylenimine solutions was estimated by measuring the temperature-dependent change of transmittance at a wavelength of 600 nm. The transmittance was measured by a V-650 UV-Vis spectrophotometer furnished with an STR-707 water thermostatted cell holder. Each sample was placed in the temperature controlled holder to be completely dissolved at a higher temperature than the phase transition temperature. Then, the temperature was lowered at a rate of 1  $^{\circ}\text{C}/\text{min}$  to observe the change of the transmittance. The phase transition temperature was defined as the temperature at which the transmittance was below 95 %.

### 3.4. Titration of *N*-sulfopropylated polyethylenimine

An acid-base titration was performed to measure the protonable

amine residues (primary, secondary, and tertiary amines) and nonprotonable quaternary ammonium residues in *N*-sulfopropylated polyethylenimine derivatives. In this titration, each sample was prepared at a concentration of 0.10 M (30 mL) in deionized water. A solution of 2 N NaOH was added to the sample to adjust the initial pH to the alkaline range. In the titration, an HCl standard solution (0.100 N) was used as the titrant to lower the pH to acidic conditions.

### 3.5. Cytotoxicity assay

MTT assay was conducted to measure the cytotoxicity of PS-PEI derivatives. HeLa (human cervical cancer) cells were seeded at  $5.0 \times 10^3$  cells/well in a 96-well plate in 90 mL DMEM containing 10% FBS, and further incubated at 37 °C for 24 h. The solution (10 mL) of each sample with various concentrations was added into the media. After incubation at 37 °C for 24 h, cells were washed with DPBS, and 20 mL filtered MTT solutions (2 mg/mL in DPBS) were added. After incubation at 37 °C for 2 h, the medium was removed and 150 mL DMSO was added to dissolve the insoluble formazan particles. The absorbance at 570 nm was measured using a microplate reader (Molecular Devices Co., Menlo Park, CA). The relative cell viability was determined as a percentage compared to the cells that were treated with buffer, which was used as the control.

## 4. Results and Discussion

### 4.1. Synthesis of *N*-sulfopropylated polyethylenimine

A variety of *N*-sulfopropylated polyethylenimine (PS-PEI) derivatives were synthesized by sulfopropylation of PEIs with different molecular weights ( $M_n = 600$  and  $1800$ ) (Fig. 1). Nucleophilic primary, secondary, and tertiary amines of the PEI backbone can attack the five-membered ring of PS to produce *N*-sulfopropylated amines or ammoniums<sup>27</sup>. PS-PEI was purified by removal of small reactants through dialysis. The  $^1\text{H}$  NMR spectra of PS-PEI are shown in Fig. 2 and Fig. 9.

The peaks of protons (d + e) in the middle methylene groups of newly introduced sulfopropyl groups are shown at 1.8-2.0 ppm. The peaks of protons (a + b) in the *b*-PEI backbone are shown at 2.4 ppm. In addition, the proton peak (f) near the quaternary ammonium residues is shown at 3.3 ppm. The degree of sulfopropylation was calculated by comparing the relative integration. The relative compositions of protonable amines and quaternary ammoniums were also calculated from the  $^1\text{H}$  NMR and  $^{13}\text{C}$  NMR (INVGATE) spectra (Fig. 10). The analyzed chemical properties of various PS-PEI derivatives are summarized in Table 1. In this study, I express the degree of sulfopropylation as a subscript and the initial  $M_n$  of *b*-PEI as a number in parentheses. For example,  $\text{PS}_{0.59}\text{-PEI}(1800)$  represents a derivative with a sulfonate to amine/ammonium (S/N) ratio of 0.59, which was synthesized from the *b*-PEI with an initial  $M_n$  of 1800.

The comparison between the degree of sulfopropylation and the amine/ammonium composition shows the difference in the reactivity of primary, secondary, and tertiary amines in *b*-PEI reactants. The majority of sulfopropylation (>97%) occurred at primary and secondary amine residues to produce secondary and tertiary amines, respectively, but the sulfopropylation at tertiary amine was rather limited, which was likely due to steric hindrance. The small proportions of quaternary ammoniums in the PS-PEI derivatives were also confirmed by  $^{13}\text{C}$  NMR INVGATE spectra (Fig. 10).

#### **4.2. Phase transition behavior of *N*-sulfopropylated polyethylenimine in water**

The Gibbs free energy of mixing ( $\Delta G_m = \Delta H_m - T\Delta S_m$ ) should be negative for the miscibility of PS-PEI in water. As the temperature ( $T$ ) increases, the negative entropy factor ( $-T\Delta S_m$ ) becomes dominant compared to the positive enthalpy factor ( $\Delta H_m$ ) in UCST mixtures, and the phase transition occurs at the temperature where  $\Delta G_m$  becomes zero. The phase transition temperature, or the cloud point ( $T_{cp}$ ), can be expressed as  $T_{cp} = \Delta H_m / \Delta S_m$ .

The phase transition temperature of PS-PEI was measured using a UV-Vis spectrophotometer. The phase-separated or insoluble particles of PS-PEI in aqueous solutions scatter the incident light to show low transmittance so that the abrupt decrease of transmittance during the cooling processes is a reasonable

estimate for the measurement of the UCST transition<sup>28</sup>.

The phase transition behavior of PS-PEI in water is shown in Fig. 3. Because the maximum aqueous solubility of PS-PEI derivatives is highly variable according to temperature, sulfopropylation degree, and molecular weight, different ranges of concentrations and temperatures were selected in the axes of Fig. 3. PS<sub>0.59</sub>-PEI(1800) is readily soluble in water at high temperatures, and the solutions have phase transition temperatures that range from 10 °C to 40 °C, according to their concentration (Fig. 3A). Another derivative with a higher degree of sulfopropylation, PS<sub>0.80</sub>-PEI(1800), showed very limited solubility in water, and the solutions have much higher phase transition temperatures that range from 65 °C to 90 °C (Fig. 3B). Conversely, the less sulfopropylated PS<sub>0.46</sub>-PEI(1800) was miscible with water at all the temperatures between 0 °C and 100 °C.

Although PS-PEI molecules contain very limited numbers of quaternary ammonium residues, which were produced by the reaction between tertiary amines and PS, they have several secondary and tertiary amine residues in their backbone (Table 1). The amines are partially protonated at neutral pH, and the degree of protonation increases as the pH decreases. The protonated amine groups can function as anchors for the interaction with negatively charged sulfonate groups, which is an important factor for the positive  $\Delta H_m$ .

As the sulfopropylation of *b*-PEI proceeded, more sulfonate residues that could interact with the protonated amine residues were introduced, and the numbers of sulfonate-protonated amine interaction were increased to result in more positive  $\Delta H_m$  values.

Consequently, PS<sub>0.80</sub>-PEI(1800) showed a higher phase transition temperature than PS<sub>0.59</sub>-PEI(1800). The  $\Delta H_m$  of the less sulfopropylated PS<sub>0.46</sub>-PEI(1800) in water was anticipated to be too small to elicit the phase transition above 0 °C.

Another important factor for the variation of the phase transition temperature is the pH value of each solution. Because of the strong acidity of sulfonic acid, the pH of the PS-PEI solution decreased with the increased degree of sulfopropylation. The pH values of PS<sub>0.46</sub>-PEI(1800), PS<sub>0.59</sub>-PEI(1800), and PS<sub>0.80</sub>-PEI(1800) were 8.5, 7.0, and 2.8, respectively. The degree of protonation of the amine residues increases as the pH decreases, which results in more positive  $\Delta H_m$  values and a higher phase transition temperature in PS-PEI with a higher degree of sulfopropylation. For a more accurate comparison, I will discuss the pH-UCST relationship in detail later.

Fig. 3C shows the effect of molecular weight on the phase transition temperature. The combinatorial factor for the  $\Delta S_m$  of a polymeric solution decreases as the molecular weight increases because the entropy that is gained during the dissolution of high molecular weight molecules is lower due to the limited degree of freedom. Therefore, a lower molecular weight derivative (PS<sub>0.82</sub>-PEI(600)) had a higher  $\Delta S_m$  than a higher molecular weight derivative (PS<sub>0.80</sub>-PEI(1800)), and it showed a lower phase transition temperature ( $\Delta H_m/\Delta S_m$ ), assuming that both derivatives have similar  $\Delta H_m$  at similar degrees of sulfopropylation. The dependence of the phase transition temperature on the molecular weight was more apparent at a similar concentration of 0.39 %wt, where PS<sub>0.82</sub>-PEI(600) and

PS<sub>0.80</sub>-PEI(1800) showed phase transition temperatures of 32 °C and 85 °C, respectively.

### 4.3. Ionic strength-UCST relationship of *N*-sulfopropylated polyethylenimine

The phase transition temperature of PS<sub>0.59</sub>-PEI(1800) at a concentration of 7.0 %wt is 27 °C in distilled water. As the ionic strength of the solution increased, the phase transition temperature gradually decreased (Fig. 4A). The UCST phase transition occurred at 1.5 °C when the NaCl concentration was 20 mM. At NaCl concentrations above 25 mM, the PS<sub>0.59</sub>-PEI(1800) was miscible with water at all the temperatures between 0 °C and 100 °C.

The enhanced miscibility was also detected in salt-added PS<sub>0.80</sub>-PEI(1800) solutions, which were difficult to be dissolved in distilled water at concentrations above 0.39 %wt. However, a 75 mM NaCl solution could dissolve concentrations of PS<sub>0.80</sub>-PEI(1800) above 10 %wt at temperatures below the phase transition temperature (85 °C). The phase transition temperature gradually decreased to 62 °C as the NaCl concentrations increased to 300 mM (Fig. 4B).

The decrease of the phase transition temperature and the increase of miscibility were mainly due to the decrease of  $\Delta H_m$  by the addition of salts. Intra- and inter-molecular attraction between zwitterionic moieties, which is an important factor for

the positive value of  $\Delta H_m$ , is generally disturbed by the addition of salts because the Debye length, the distance at which opposite charges sense each other in solutions, decreases according to the equation  $l_D = (4\pi \cdot l_B \cdot c_s)^{-0.5}$ , where  $l_B$  and  $c_s$  are the Bjerrum length in pure water and the salt concentration, respectively<sup>25</sup>. The decrease of electrostatic attraction by the addition of salts caused  $\Delta H_m$  to be less positive, resulting in the decrease of the UCST phase transition temperature and the increase of miscibility.

#### **4.4. pH-UCST relationship of *N*-sulfopropylated polyethylenimine**

UCST transition is dependent upon concentration, pH, and ionic strength. To examine the effect of pH on UCST more accurately, I checked the phase transition of PS-PEI(1800) in solutions with different pH values at fixed concentrations and ionic strengths (Fig. 5).

As shown in Fig. 4, PS<sub>0.59</sub>-PEI(1800) solutions with more than 25 mM NaCl did not exhibit a UCST phase transition at pH 7.0. However, as the pH of the solution decreased, the UCST transition appeared and the phase transition temperature gradually increased. Even in the presence of 90 mM NaCl, phase transition temperatures of 49 °C and 88 °C were observed at pH 6.0 and 5.0, respectively (Fig. 5A).

PS<sub>0.46</sub>-PEI(1800) was miscible with water without any additional



salts at pH 8.5 between 0 °C and 100 °C (Table 1). As the pH decreased, the miscibility was markedly decreased to show the UCST phase transition. At pH 6.3 and a NaCl concentration of 122 mM, PS<sub>0.46</sub>-PEI(1800) showed an abrupt change of miscibility at 19 °C. Phase transition temperatures of 55 °C and 68 °C were observed at pH 4.9 and 3.0, respectively (Fig. 5B).

The strong pH dependence of the UCST phase transition of PS-PEI originated from the pH-dependent protonation of primary, secondary, and tertiary amines in the PEI backbone. Because only a limited amount of quaternary ammoniums were produced by the sulfopropylation of *b*-PEI (Table 1), the numbers of protonable amines were almost unchanged. The protonation behavior of PS-PEI derivatives according to pH is shown in Fig. 6. PS-PEI derivatives showed similar protonation behaviors with *b*-PEI, which has a wide buffering range from pH 11 to pH 3. Considering the strong acidity of the sulfonate residues that were generated ( $pK_a \sim 2$ ), the buffering that is shown in Fig. 6 was mostly caused by the protonation of primary, secondary, and tertiary amines of the PS-PEI derivatives. Consequently, the sulfonate residues remained almost negatively charged within the pH range that is shown in Fig. 5, but the amine residues gradually became positively charged during the acidification.

At high pH values, the ratio of positively charged ammoniums, which can interact with negatively charged sulfonates, was quite limited. The limited interaction could not provide adequate positive  $\Delta H_m$  for the UCST phase transition, and the PS-PEI derivatives were miscible with water regardless of the temperature. As the protonation of amine residues increased

during acidification, the intra- or inter-molecular interaction between ammonium and sulfonate residues increased to show the phase separation of PS-PEI from water below a certain temperature. The phase transition temperature increased as the  $\Delta H_m$  increased during the acidification. At very low pH, the  $\Delta H_m$  from the electrostatic interactions was too positive, and the mixing between the two phases (negative  $\Delta G_m$ ) could only be observed at a very high temperature; it was not observed below the boiling point of water. The proposed mechanism of the phase separation is illustrated as a simplified schematic diagram in Fig. 7.

#### 4.5. Cytotoxicity assay

For future applications in the biomedical field, the cytotoxicity of PS-PEI was examined by MTT assay. Fig. 8 shows the relative viability of HeLa cells that were treated with PS-PEI derivatives. Although high-molecular weight PEI (>25 kDa) is notorious for its high cytotoxicity<sup>29</sup>, low-molecular-weight PEI (<2 kDa) showed relatively marginal toxicity with approximately 80 % cell viability at concentrations between 20 mg/mL and 100 mg/mL. The *N*-sulfopropylated PEI showed even lower cytotoxicity than *b*-PEI (1800), and PS<sub>0.80</sub>-PEI(1800) showed almost 100% cell viability. It was hypothesized that the cytotoxicity of PEI was due to the strong interaction of rich amine residues in the PEI backbone with cell membranes or chromosomes<sup>30</sup>. Therefore, the reduction of cytotoxicity of PS-PEI was reasonable because the

harmful interaction could be partially impaired by the electrostatic interaction with the neighboring sulfonate residues.

## 5. Conclusions

In summary, I introduced UCST properties into a pre-existing biopolymer, *b*-PEI, by a simple sulfopropylation reaction. The presence of large amounts of protonable amine residues in PS-PEI backbones can increase the enthalpy of mixing, demonstrating the strong pH dependence of the UCST phase transition. Given the various applications of *b*-PEI and the low cytotoxicity of PS-PEI, the precise control of UCST phase transition by pH and the degrees of sulfopropylation could have a significant impact on the drug delivery of biomaterials that are sensitive to temperature and pH.

## 6. References

1. AP. Kryvoruchko, L. Yu, ID. Atamanenko and BY. Kornilovic, *Desalination*, 2004, 162, 229.
2. J. Woodard, *Soc Cosmet Chem*, 1972, 23, 593.
3. B. Alince, A. Vanerek and TGM. van de Ven, *J. Pulp. Pap. Sci.*, 2002, 28, 315.
4. Y. Lee, MY. Cho, H. Mo, K. Nam, H. Koo and GW. Jin. B. *Korean. Chem. Soc.*, 2008, 29, 666.
5. X. Yang, Y. Peng, B. Yu, J. Yu, C. Zhou and Y. Mao, *Mol. Pharmaceutics.*, 2011, 8, 709.
6. S. Werth, B. Urba-Klein, L. Dai, S. Höbel, M. Grzelinski and U. Bakowsky, *J. Control. Release.*, 2006, 112, 257.
7. O. Boussif, F. Lezoualch, MA. Zanta, MD. Mergny, D. Scherman and B. Demeneix, *P. Natl. Acad. Sci.*, 1995, 92, 7297.
8. YH. Wang, M. Zheng, FH. Meng, J. Zhang, R. Peng and ZY. Zhong, *Biomacromolecules*, 2011, 12, 1032.
9. Y. Lee and K. Kataoka, *Soft Matter.*, 2009, 5, 3810.
10. JQ. Jiang, X. Tong and Y. Zhao, *J. Am. Chem. Soc.*, 2005, 127, 8290.
11. N. Rapoport, *Prog. Polym. Sci.*, 2007, 32, 962.
12. HS. Bisht, DS. Manickam, YZ. You and D. Oupicky, *Biomacromolecules*, 2006, 7, 1169.

13. A. Harada and K. Kataoka, *J. Macromol. Sci. Pure.*, 1997, A34, 2119.
14. Y. Lee, H. Mo, H. Koo, JY. Park, MY. Cho and GW. Jin, *Bioconjugate Chem.*, 2007, 18, 13.
15. SV. Solomatin, TK. Bronich, TW. Bargar, A. Eisenberg, VA. Kabanov and AV. Kabanov, *Langmuir*, 2003, 19, 8069.
16. H. Kasai, T. Murakami, Y. Ikuta, Y. Koseki, K. Baba and H. Oikawa, *Angew. Chem. Int. Edit.*, 2012, 51, 10315.
17. D. Pissuwan, SM. Valenzuela and MB. Cortie, *Trends. Biotechnol.*, 2006, 24, 62.
18. P. Diagaradjane, A. Shetty, JC. Wang, AM. Elliott, J. Schwartz and S. Shentu, *Nano. Lett.*, 2008, 8, 1492.
19. R. Yoshida, K. Uchida, Y. Kaneko, K. Sakai, A. Kikuchi and Y. Sakurai, *Nature*, 1995, 374, 240.
20. J. Seunng and S. Agarwal, *Macromolecules*, 2012, 45, 3910.
21. H. Kim, S. Lee, M. Noh, SH. Lee, Y. Mok, GW. Jin, J. Seo and Y. Lee, *Polymer*, 2011, 52, 1367.
22. H. Kakuda, T. Okada and T. Hasegawa, *J. Phys. Chem. B*, 2009, 113, 13910.
23. H. Yoshimitsu, A. Kanazawa, S. Kanaoka and S. Aoshima, *Macromolecules*, 2012, 45, 9427.
24. DN. Schulz, DG. Peiffer, PK. Agarwal, J. Larabee, Kaladas JJ and L. Soni, *Polymer*, 1986, 27, 1734.
25. P. Mary, DD. Bendejacq, MP. Labeau and P. Dupuis, *J. Phys.*

Chem. B, 2007, 111, 7767.

26. J. Seuring and S. Agarwal, *Macromol. Rapid Commun.*, 2012, 33, 1898.

27. Natus. Guy and Goethals. Eric, *Macromol. Rapid Commun.*, 1969, 123, 130.

28. DE. Bergbreiter and H. Fu, *J. Polym. Sci. Polym. Chem.*, 2008, 46, 186.

29. Y. Lee and K. Kataoka, *Adv. Polym. Sci.*, 2012, 249, 95.

30. N. Oku, N. Yamaguchi, N. Yamaguchi, S. Shibamoto, F. Ito and M. Nango, *J. Biochem. Tokyo.*, 1986, 100, 935.

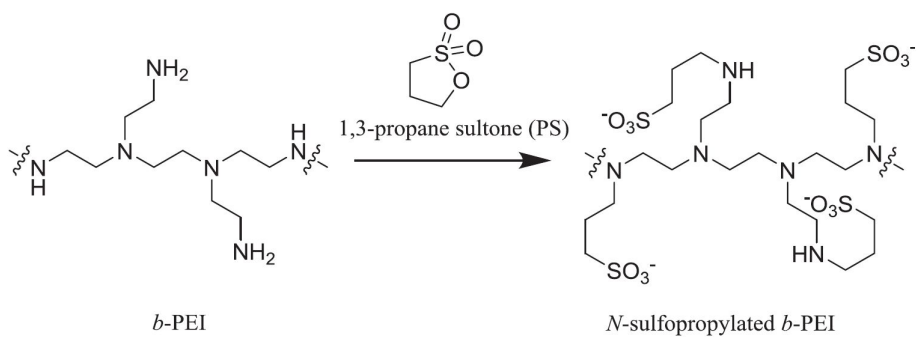


**Figure 1.** Synthetic scheme of *N*-sulfopropylated *b*-PEI.



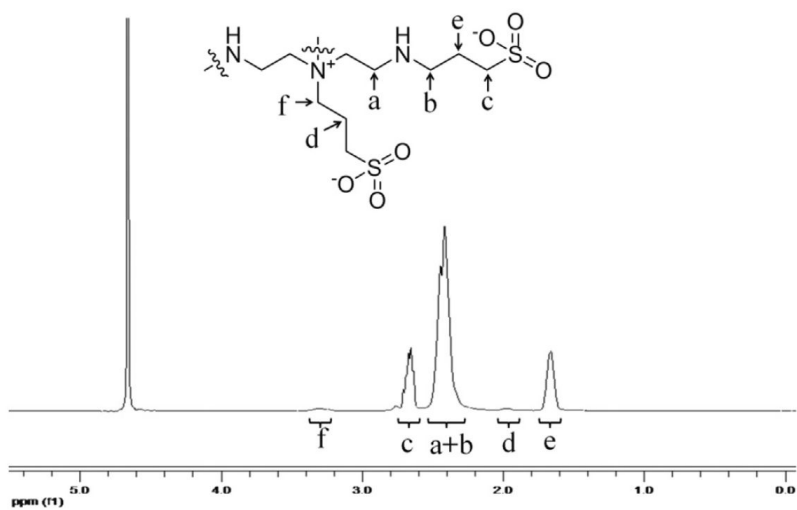


**Figure 2.**  $^1\text{H}$  NMR spectrum of  $\text{PS}_{0.59}\text{-PEI}$  (1800) in  $\text{D}_2\text{O}$  (0.97%  $\text{NaOD}$ ).

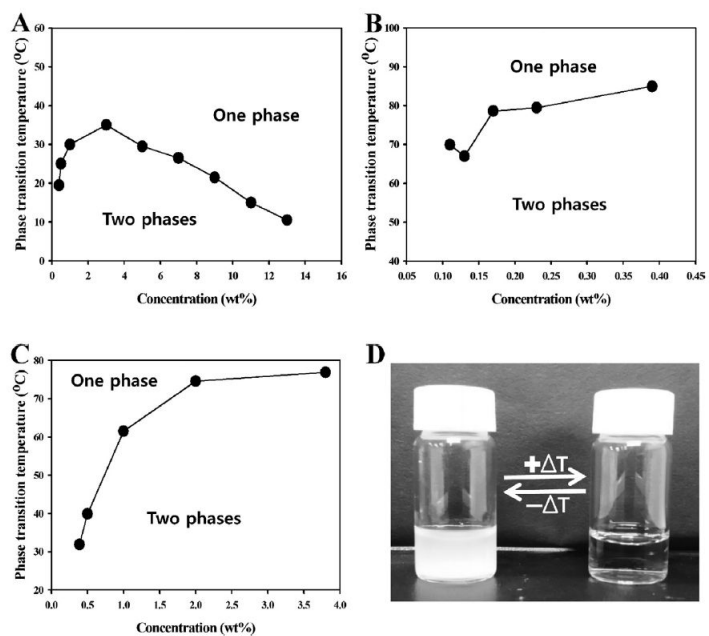


**Figure 3.** Phase diagram of (A) PS<sub>0.59</sub>-PEI(1800), (B) PS<sub>0.80</sub>-PEI(1800), and (C) PS<sub>0.82</sub>-PEI(600) in water. (D) UCST transition of 5.0 %wt PS<sub>0.59</sub>-PEI(1800).

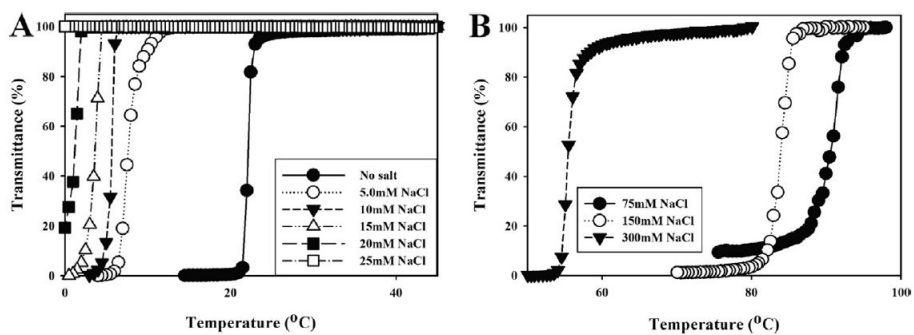


**Figure 4.** Effect of ionic strength on the phase transition temperature of (A) PS<sub>0.59</sub>-PEI(1800) (7.0 %wt; pH 7.0) and (B) PS<sub>0.80</sub>-PEI(1800) (10 %wt; pH 2.8).

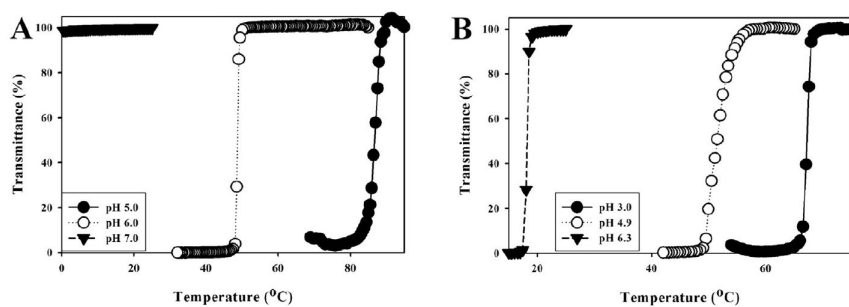


**Figure 5.** Effect of pH on the phase transition temperature of (A) PS<sub>0.59</sub>-PEI(1800) (7.0 %wt; 90 mM NaCl) and (B) PS<sub>0.46</sub>-PEI (1800) (5.0 %wt; 122 mM NaCl).

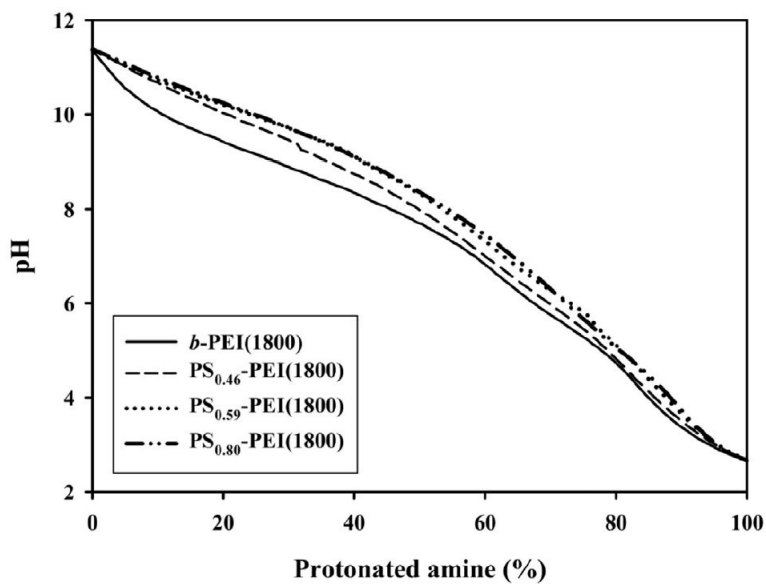


**Figure 6.** Comparison of buffering capacity of *b*-PEI(1800), PS<sub>0.46</sub>-PEI(1800), PS<sub>0.59</sub>-PEI(1800), and PS<sub>0.80</sub>-PEI(1800) at varying pH values.

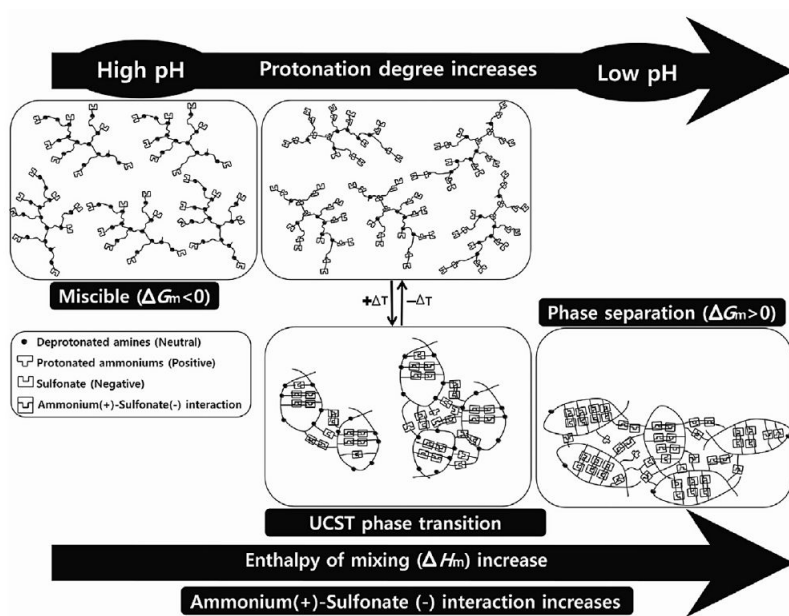


**Figure 7.** The proposed mechanism of the pH-dependent UCST phase separation of PS-PEI derivatives.

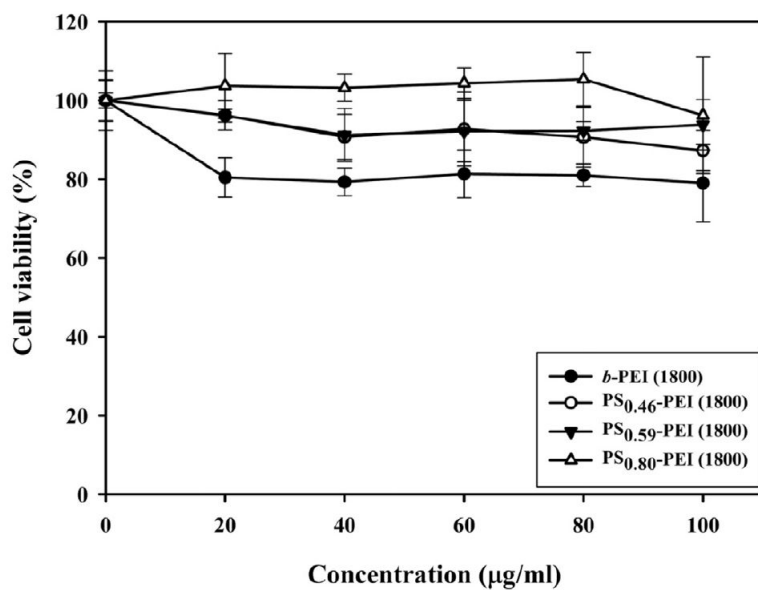


**Figure 8.** Relative viability of HeLa cells treated with PS-PEI derivatives. Each data point represents the average value of four experiments ( $\pm$ S.D.).

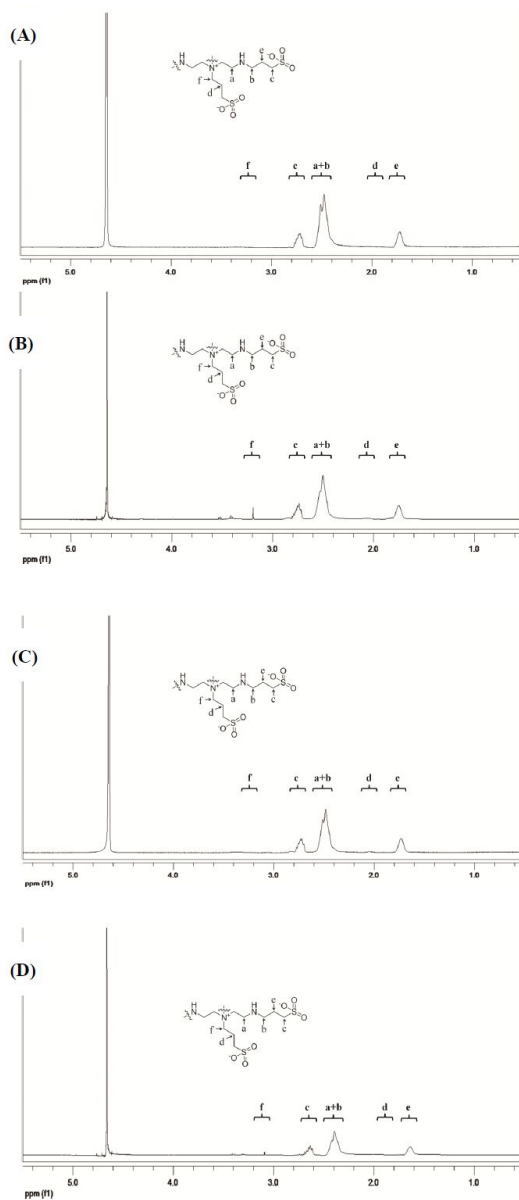


**Figure 9.**  $^1\text{H}$  NMR spectra of  $\text{PS}_{0.46}\text{-PEI}(1800)$  (A),  $\text{PS}_{0.80}\text{-PEI}(1800)$  (B),  $\text{PS}_{0.60}\text{-PEI}(600)$  (C), and  $\text{PS}_{0.82}\text{-PEI}(600)$  (D) in  $\text{D}_2\text{O}$  (0.97 wt% NaOD).



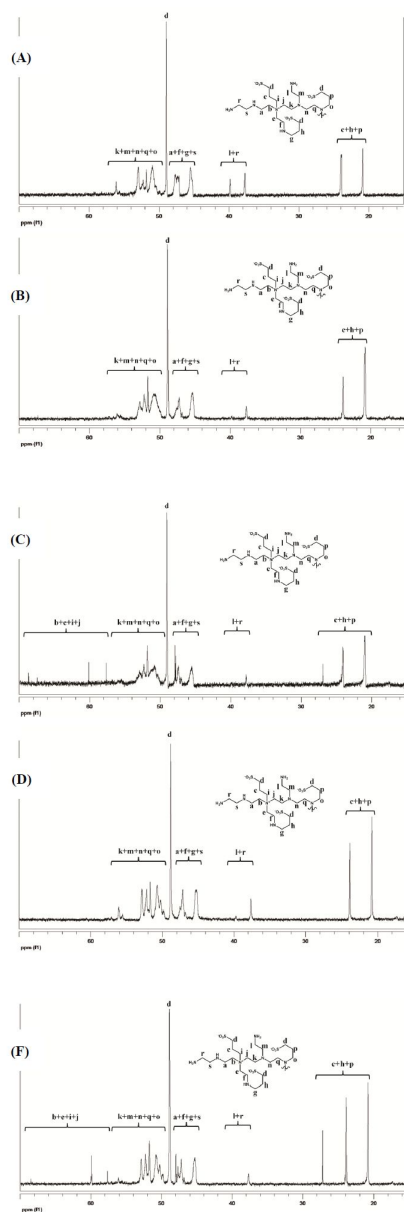


**Figure 10.**  $^{13}\text{C}$  NMR INVGATE spectra of  $\text{PS}_{0.46}\text{-PEI}(1800)$  (A),  $\text{PS}_{0.59}\text{-PEI}(1800)$  (B),  $\text{PS}_{0.80}\text{-PEI}(1800)$  (C),  $\text{PS}_{0.60}\text{-PEI}(600)$  (D), and  $\text{PS}_{0.82}\text{-PEI}(600)$  (E) in  $\text{D}_2\text{O}$  (0.97 wt% NaOD).

**Table 1.** Synthesized PS-PEI derivatives.

	PS/N ratio in reactants	S/N ratio in PS-PEI <sup>a</sup>	% of protonable amines <sup>b</sup>	Phase transition temperature <sup>c</sup> (°C)
PS-PEI(1800)	0.50	0.46	100	–
	1.0	0.59	100	19
	2.0	0.80	97.9	85
PS-PEI(600)	1.0	0.62	100	–
	2.0	0.82	98.3	32

<sup>a</sup> Sulfonate(S) to amine/ammonium (N) ratios in PS-PEI were determined by <sup>1</sup>H NMR.

<sup>b</sup> Relative composition of protonable amines was determined by <sup>1</sup>H NMR and <sup>13</sup>C NMR.

<sup>c</sup> The phase transition temperature was measured at the concentration of 0.39 %wt in distilled water.

### Part III. Upper critical solution temperature (UCST) phase transition of halide salts of branched polyethylenimine and methylated branched polyethylenimine in aqueous solutions

#### 1. Abstract

The upper critical solution temperature (UCST) phase transition of halide salts of branched polyethylenimine (PEI) and methylated branched polyethylenimine (MPEI) is first reported in aqueous solutions. In particular, iodide counter-ions can introduce UCST properties in MPEI. The importance of the counter-ion composition of MPEI for UCST transition is discussed in detail.

## 2. Introduction

Polymers with temperature responsiveness have been extensively researched in the past decades. The temperature-responsive phase transition arises from different interactions between polymer and solvent molecules according to temperature variation. In a lower critical solution temperature (LCST) mixture, a polymer is miscible with a solvent below a certain temperature, but it is abruptly phase-separated above that temperature. On the other hand, an upper critical solution temperature (UCST) polymer-solvent mixture exhibits phase separation below the phase transition temperature. In particular, such phenomena in aqueous mixtures have been used in various fields, including hydrogels,<sup>1</sup> drug delivery,<sup>2</sup> chromatography,<sup>3</sup> water purification,<sup>4</sup> and optical devices.<sup>5</sup>

In many cases, UCST phase transition occurs when solute-solute or solvent-solvent interactions dominate the solute-solvent interaction to generate the positive enthalpy of mixing ( $\Delta H_m < 0$ ), unlike LCST phase transitions, which are more dependent upon the negative entropy of mixing ( $\Delta S_m < 0$ ) due to the strong solute-solvent interaction.<sup>6</sup> In aqueous solution, examples of UCST polymers have been reported less frequently than those of LCST polymers, partially due to the characteristic strong interaction between polymers and water molecules with strong polarity and hydrogen-bonding capability.<sup>7</sup> Some selective polymers with hydrogen-bond-forming residues, such as urea<sup>8</sup> and amide,<sup>9</sup> or zwitterion residues, such as sulfopropyl ammonium<sup>10</sup> and sulfopropyl imidazolium,<sup>11</sup> exhibit UCST properties in water because the strong polymer-polymer

interaction can overcome the polymer - water interaction to generate positive  $\Delta H_m$ . It was also reported that complex coacervate micelles composed of oppositely charged polymeric ions showed UCST-like behaviour in aqueous solutions.<sup>12</sup>

Because the strong electrostatic interaction between polymer residues can induce UCST phase transition, I hypothesized that simple polymer - monomeric ion salts, not zwitterionic polymers or oppositely charged polymeric ion-based coacervates, could also exhibit a similar transition in aqueous solution. Of course, a separate monomeric ion salt has a larger positive statistical  $\Delta S_m$  due to a larger increase of the degree of freedom during the solvation process compared to the corresponding zwitterion or polymer - polymer ion salt. Because the phase transition occurs when the Gibbs free energy of mixing ( $\Delta G_m = \Delta H_m - T\Delta S_m$ ) becomes zero at a certain polymer - ion salt/water composition,<sup>13</sup> the phase transition temperature ( $T = \Delta H_m/\Delta S_m$ ) of the separate polymer - monomeric ion salt might be lower than that of the zwitterionic or polymer - polymer ion salt if I assume that other conditions are the same in both polymers. Therefore, if I want to arrange,  $\Delta H_m$  should be increased to compensate for the increase of  $\Delta S_m$ .

### 3. Materials and Methods

#### 3.1. Materials

Two branched polyethylenimine (*b*-PEI) polymers ( $M_w = 25,000$  ( $PD(M_w/M_n) = 2.5$ ) or  $M_w = 800$  ( $PD(M_w/M_n) = 1.3$ )), iodomethane ( $\text{CH}_3\text{I}$ ) and *N,N*-diisopropylethylamine, sodium bromide (NaBr), sodium thiocyanate (NaSCN) and sodium tetrafluoroborate ( $\text{NaBF}_4$ ) were purchased from Aldrich (USA). Ethanol, *N,N*-dimethylformamide (DMF), ammonium hydroxide ( $\text{NH}_4\text{OH}$ ), sodium hydroxide (NaOH) and sodium chloride (NaCl) were purchased from Daejung (Korea). All reagents were used without further purification.

#### 3.2. Synthesis of methylated polyethylenimine halide

A solution of *b*-PEI ( $M_w = 25,000$  ( $PD(M_w/M_n) = 2.5$ ) or  $M_w = 800$  ( $PD(M_w/M_n) = 1.3$ )) in DMF was added to a stirred solution of *N,N*-diisopropylethylamine in DMF at 30 °C.  $\text{CH}_3\text{I}$  (5.0 eq. of total amines in *b*-PEI) was slowly added to the solution. After 48 h of stirring, ammonium hydroxide solution was added to the solution for quenching. For the purification of MPEII (25 kDa), the reaction mixture was dialyzed against ethanol ( $\times 3$ ) and deionized water ( $\times 5$ ) using a membrane (MWCO = 6 - 8 kDa). MPEII (0.80 kDa) was purified by ethanol precipitation. The purified MPEII was lyophilized to obtain the

product as a pale yellow powder. The structure was characterized using the inverted gate (INVGATE)  $^{13}\text{C}$  NMR technique (Agilent 400-MR DD2 (400 MHz)). Other MPEI salts were obtained by excessive dialysis of MPEII against corresponding sodium salt solutions (NaCl, NaBr, NaSCN, or  $\text{NaBF}_4$ ).

### 3.3. Measurement of the UCST phase transition

The phase transition was monitored by a V-650 UV-Vis spectrophotometer (Jasco, Japan) equipped with an STR-707 water thermostatted cell holder. Each sample was completely dissolved in aqueous solution above the phase transition temperature and then positioned in the temperature-controlled holder. The phase transition temperature was determined as the temperature showing 50 % of the transmittance when the cooling rate was set at 1  $^{\circ}\text{C}/\text{min}$ . For the adjustment of total anionic concentration in Fig. 3A, NaCl and NaI were added to the mixture of MPEII and MPEIC at a specific  $[\text{I}^-]/[\text{A}^-]$  ratio.

## 4. Results and Discussion

### 4.1. Phase transition behavior of various polyethylenimine halide salts

As a model polymer backbone for UCST transition, I chose branched polyethylenimine (*b*-PEI) with a high amine density (1 amine residue per 43 Da). Primary, secondary, and tertiary amines of *b*-PEI were gradually protonated with the addition of hydrogen halide, and the resulting ammonium residues could interact with halide counter-ions (Fig. 1A). If the interaction was strong enough to overcome the water-ion interaction, a positive  $\Delta H_m$  could be generated to show UCST phase transition. As shown in Fig. 1 and Fig. 4, various polyethylenimine (PEI) halide salts exhibited UCST phase transition in the temperature range between 0 °C and 50 °C. UCST phase transition of the PEI halide is quite sensitive to the amount of hydrogen halide. The phase transition temperature of PEI bromide (PEIB) increased as the HBr/amine (N) ratio increased (Fig. 1B). Excessive HBr might have induced the further protonation of internal tertiary amines in PEI,<sup>14</sup> and the electrostatic interaction between ammonium and halide ions increased to elevate  $\Delta H_m$  and the phase transition temperature. Excessive HBr might also elevate the phase transition temperature by the salting-out type effect. The phase transition temperature of PEIB was also dependent on the composition (Fig. 1C). Both PEI chloride (PEIC) and PEI iodide (PEII) exhibited the UCST phase transition, although it was



observed in a very narrow range of the composition and halide/N ratio (Fig. 4). The UCST phase transition of simple polymer-halide salts in aqueous solutions is reported here for the first time, although the UCST phase transition of polymer-complex ions was reported in a few previous papers.<sup>15</sup>

#### 4.2. Preparation of methylated polyethylenimine halide

However, the UCST phase transition of the PEI halide can be observed only under extreme pH conditions (Table 1), probably because a considerable number of cationic ammonium residues, which interact with halide anions, can be generated only under those conditions. To obtain polymeric salts, which can show the UCST phase transition under more tolerable conditions, I prepared a methylated PEI possessing permanent cationic ammonium residues irrespective of pH conditions (Fig. 2A). The methylated polyethylenimine iodide (MPEII) was prepared by the nucleophilic substitution between primary, secondary, and tertiary amine residues of *b*-PEI and methyl iodide (CH<sub>3</sub>I).<sup>16</sup> The quaternary ammonium degree of each polymer salt was determined using the inverted gate (INVGATE) <sup>13</sup>C NMR technique.<sup>17</sup> I could obtain an MPEII of which 35 - 38 % of the total amine residues were quaternized (MPEII<sub>0.35</sub> or MPEII<sub>0.38</sub>) using the 5.0 equivalents of CH<sub>3</sub>I (Fig. 5). Most of the quaternary ammoniums originated from more-exposed primary amines on the external part of *b*-PEI through methylation reactions. Excess iodide salts were removed or exchanged with

chloride or bromide to produce methylated polyethylenimine chloride (MPEIC) or bromide (MPEIB) by dialysis (Fig. 2A).

#### 4.3. Phase transition behavior of methylated polyethylenimine halide

Interestingly, unlike the unmethylated correspondents, only MPEII exhibited UCST phase transition in the temperature range of 0 - 20 °C (Fig. 2B). Marginal hysteresis ( $\Delta T \approx 1 - 2$  °C) was observed in the phase transition of MPEII (Fig. 6), which is a typical characteristic of temperature-sensitive phase transition of polymers.<sup>18</sup> Both MPEIC and MPEIB are miscible with water in the temperature range of 0 - 100 °C. In the case of MPEI, the hydrophobic interaction between the methylated ammonium residues ( $\text{NR}_4^+$ ) and the halide ions might have been an important factor as also the electrostatic interaction. The molar Gibbs free energies of the hydration of  $\text{Cl}^-$ ,  $\text{Br}^-$  and  $\text{I}^-$  are -340, -315, and -275 kJ/mol, respectively.<sup>19</sup> Due to the more hydrophobic character of I compared with other halide ions, the interaction of  $\text{I}^-$  with  $\text{NR}_4^+$  is fairly higher than  $\text{Cl}^-$  and  $\text{Br}^-$ .<sup>20</sup> The stronger interaction between  $\text{NR}_4^+$  and  $\text{I}^-$  can dominate the interaction between water molecules and ions to generate positive  $\Delta H_m$  and give the UCST properties to MPEII. However, the water-ion interaction might be stronger than the weaker interaction between  $\text{NR}_4^+$  and other halide ions to generate negative  $\Delta H_m$  and negative  $\Delta G_m (= \Delta H_m - T\Delta S_m)$  in the temperature range.

The composition - temperature phase diagram of MPEII/water

mixtures showed a typical convex shape that has been observed in many other UCST mixtures (Fig. 2C).<sup>21</sup> Fig. 2C also shows the effect of molecular weight on the phase transition temperature. High-molecular-weight MPEII<sub>0.35</sub> (25 kDa) has a higher phase transition temperature than low-molecular-weight MPEII<sub>0.38</sub> (0.80 kDa). High-molecular-weight MPEII has a less-positive  $\Delta S_m$  than low-molecular-weight MPEII due to a smaller combinatorial entropy gain during mixing. Therefore, MPEII<sub>0.35</sub> (25 kDa) showed a higher phase transition temperature ( $T = \Delta H_m / \Delta S_m$ ) than MPEII<sub>0.38</sub> (0.80 kDa), assuming that both derivatives have a similar  $\Delta H_m$  at similar degrees of quaternization (35 % vs. 38 %).

#### **4.4. Effect of counterions in methylated polyethylenimine backbone**

To investigate the effect of counter-ions, the phase transition of MPEI halide was observed by varying the counter-ion composition and total anion concentrations ( $[A^-] = [I^-] + [Cl^-]$ ) (Fig. 3A). When only  $I^-$  existed as the counterion ( $[I^-]/[A^-] = 100\%$ ), the phase transition temperature increased until the total anion concentration ( $[A^-]$ ) was 2.00 M and decreased above that concentration. The elevation of phase transition temperature at lower anion concentrations ( $<2.00$  M) indicated the increase of the polymer-ion interaction. Similar to the salting-out effect, the increased ionic strength might strengthen the hydrophobic interaction between ammonium and  $I^-$  in this range of

concentrations. However, at higher anion concentrations ( $>2.00$  M), the reduction of electrostatic interaction by the decreased Debye length might have dominated the increased hydrophobic interaction to exhibit the salting-in type phenomena of MPEI halide. The former salting-out effect seemed to be dominant when  $\text{Cl}^-$  co-existed with  $\text{I}^-$ . Generally, smaller and more hydrophilic ions, such as  $\text{Cl}^-$ , exhibit a stronger salting-out effect than larger and more hydrophobic ions, such as  $\text{I}^-$ .<sup>22</sup> Therefore, the phase transition temperature increased as the total anion concentration increased when the  $\text{I}^-$  content ( $[\text{I}^-]/[\text{A}^-]$ ) was lower than 90 %, although no salting-out was observed with an  $[\text{A}^-]$  greater than 2.25 M. Meanwhile, the phase transition temperature decreased as the  $\text{I}^-$  content decreased below 90 %, and the phase separation could not be observed at the  $\text{I}^-$  content below 70 %. This result clearly supports the importance of the interaction between  $\text{NR}_4^+$  and hydrophobic  $\text{I}^-$  in MPEI for obtaining the UCST properties. With an  $\text{I}^-$  content of between 100 % and 90 %, the stronger salting-out effect of  $\text{Cl}^-$  and the stronger  $\text{NR}_4^+ - \text{I}^-$  interaction competed with each other to show a rather complex intersection of graphs.

To investigate the effect of the hydrophobicity of counterions in MPEI on UCST phase transition behaviour, the  $\text{I}^-$  of MPEII was replaced with other hydrophobic anions, such as thiocyanate ( $\text{SCN}^-$ ) or tetrafluoroborate ( $\text{BF}_4^-$ ), of which the molar Gibbs free energies of hydration are  $-280$  and  $-190$  kJ/mol, respectively.<sup>19</sup> As shown in Fig. 3B, the tetrafluoroborate salt of MPEI ( $\text{MPEI}(\text{BF}_4)_{0.35}$ ) exhibited a UCST phase transition with higher phase transition temperatures than  $\text{MPEII}_{0.35}$ . The stronger hydrophobicity of  $\text{BF}_4^-$  over  $\text{I}^-$  would contribute to the elevation

of the phase transition temperature in aqueous solutions. Interestingly, even though the molar Gibbs free energies of hydration of  $\text{SCN}^-$  is similar to that of  $\text{I}^-$ , the thiocyanate salt of MPEI ( $\text{MPEI}(\text{SCN})_{0.35}$ ) did not exhibit the UCST phase transition and was miscible with water in the temperature range of 0 - 100 °C. It is probable that other characteristics of anions would affect the interaction with MPEI polymers. However, the hydrophobicity of counter-anions seemed to be an important factor for the introduction of the UCST properties into alkylated quaternary ammonium polymers.

## 5. Conclusions

In conclusion, I demonstrated that simple polymer-ion salts such as the halide salts of PEI and MPEI could show the UCST phase transition in aqueous solutions if the polymer-ion interaction is strong enough to overcome the solute-water interaction. Without the complex synthesis of polymers containing zwitterionic or hydrogen bonding moieties, the simple exchange of counter-ions or methylation could introduce the UCST properties into pre-existing polymers. After conducting future research studies involving the variation of the cationic and anionic parts of polymers and ions, the characteristics of temperature-responsive polymeric salts will be understood in more detail, and they will be more helpful in the development of practical temperature-responsive smart materials for various applications.

## 6. References

1. B. Guo, G. Pan, Q. Guo, C. Zhu, W. Cui, B. Li and H. Yang, *Chem. Commun.*, 2015, 51, 644.
2. A. Rahikkala, V. Aseyev, H. Tenhu, E. I. Kauppinen and J. Raula, *Biomacromolecules*, 2015, 16, 2750.
3. M. Lee, E. S. Chan, K. C. Tam and B. T. Tey, *J. Chromatogr. A*, 2015, 1394, 71.
4. M. Noh, Y. Mok, S. Lee, H. Kim, S. Lee, G. Jin, J. Seo, H. Koo, T. Park and Y. Lee, *Chem. Commun.*, 2012, 48, 3845; J. P. A. Custers, S. F. G. M. Nispen, A. Can, V. R. Rosa, S. Maji, U. S. Schubert, J. T. F. Keurentjes and R. Hoogenboom, *Angew. Chem., Int. Ed.*, 2015, DOI: 10.1002/anie.201505351.
5. S. Asher, J. Weissman and H. Sunkura, US Pat., 6165389, University of Pittsburgh of the Commonwealth of Higher Education, 2000.
6. Q. Zhang and R. Hoogenboom, *Prog. Polym. Sci.*, 2015, 48, 122.
7. J. Seuring and S. Agarwal, *Macromol. Rapid Commun.*, 2012, 33, 1898.
8. A. Fujihara, N. Shimada, A. Maruyama, K. Ishihara, K. Nakai and S. Yusa, *Soft Matter*, 2015, 11, 5204.
9. J. Seuring, F. Bayer, K. Huber and S. Agarwal, *Macromolecules*, 2012, 45, 374.
10. Z. A. Jiménez and R. Yoshida, *Macromolecules*, 2015, 48,

4599.

11. V. A. Vasantha, S. Jana, A. Parthiban and J. G. Vancso, *Chem. Commun.*, 2014, 50, 46.
12. N. Bourouina, M. A. C. Stuart and J. M. Kleijn, *Soft Matter*, 2014, 10, 320.
13. H. Yoshimitsu, A. Kanazawa, S. Kanaoka and S. Aoshima, *Macromolecules*, 2012, 45, 9427.
14. S. Lee, S. Kim, S. Hah and J. Suh, *Bioorg. Chem.*, 1997, 25, 221.
15. F. A. Plamper, A. Schmalz, M. Ballauff and A. H. E. Müller, *J. Am. Chem. Soc.*, 2007, 129, 14538; Q. Zhang and J. Hong, Richard Hoogenboom, *Polym. Chem.*, 2013, 4, 4322.
16. L. Atar-Froyman, A. Sharon, E. I. Weiss, Y. Hourí-Haddad, D. Kesler-Shvero, A. J. Domb, R. Pilo and N. Beyth, *Biomaterials*, 2015, 46, 141.
17. Y. Lim, S. Kim, Y. Lee, W. Lee, T. Yang, M. Lee, H. Suh and J. Park, *J. Am. Chem. Soc.*, 2001, 123, 2460.
18. J. Seuring and S. Agarwal, *Macromolecules*, 2012, 45, 3910.
19. Y. Marcus, *J. Chem. Soc., Faraday Trans.*, 1991, 87, 2995.
20. J. Heyda, M. Lund, M. Onca'k, P. Slavý'cek and P. Jungwirth, *J. Phys. Chem. B*, 2010, 114, 10843.
21. M. Noh, Y. Mok, D. Nakayama, S. Jang, S. Lee, T. Kim and Y. Lee, *Polymer*, 2013, 54, 5338.
22. Y. Zhang, S. Furyk, D. Bergbreiter and P. Cremer, *J. Am.*



Chem. Soc., 2005, 127, 14505.

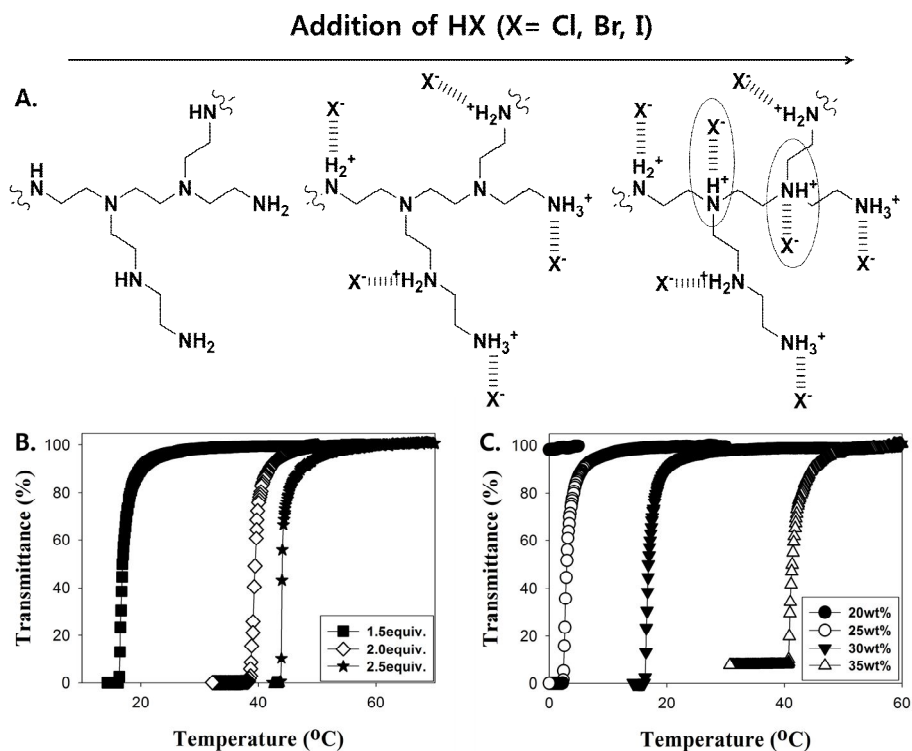


**Figure 1.** (A) Interaction between ammonium residues and halide counterions in PEI halide salts. (B) Phase transition of PEIB at 30 % (w/w) polymer composition at various ratios of HBr/N ratio (C) Phase transition of PEIB at various compositions, HBr/N ratio of 1.5.



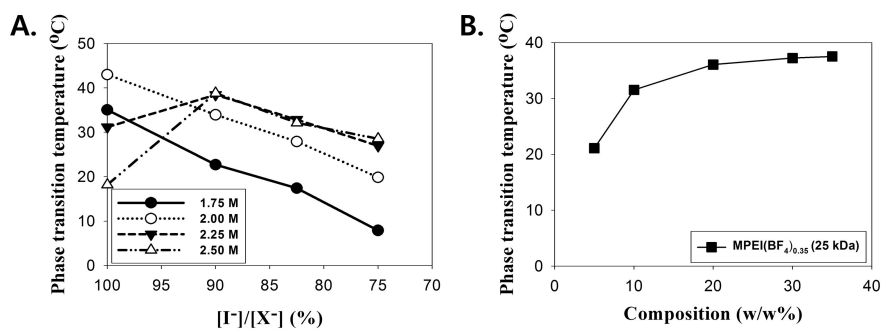


**Figure 3.** (A) Change of phase transition temperature of MPEI<sub>0.35</sub> (25 kDa) at various counter-ion composition and the total anion concentration. (B) Composition - temperature phase diagram of MPEI(BF<sub>4</sub>)<sub>0.35</sub> (25 kDa).

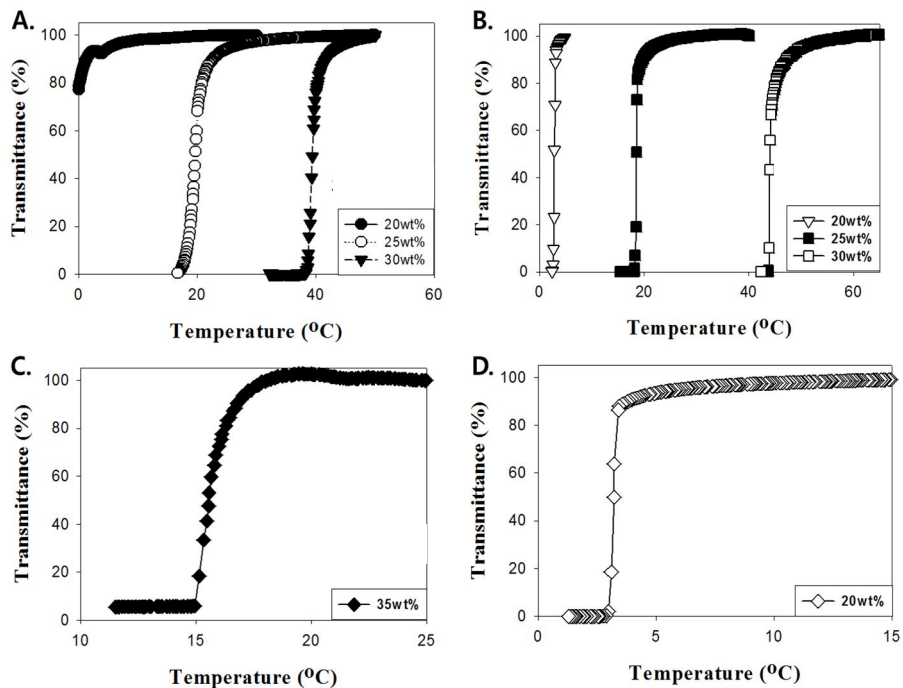
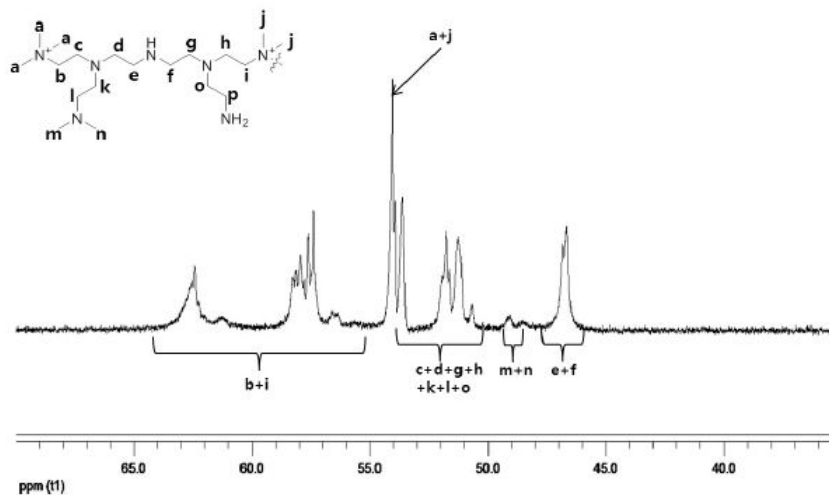


**Figure 4.** (A) Phase transition behavior of PEIB at HBr/N ratio or 2. (B) Phase transition behavior of PEIB at HBr/N ratio or 2.5 . (C) Phase transition behavior of PEII at a polymer composition of 35 % (w/w) and HI/N ratio of 1.5. (D) Phase transition behavior of PEIC at a polymer composition of 20 % (w/w) and HCl/N ratio of 4.0.

A. MPEII<sub>0.35</sub> (25 kDa)



B. MPEII<sub>0.38</sub> (0.80 kDa)

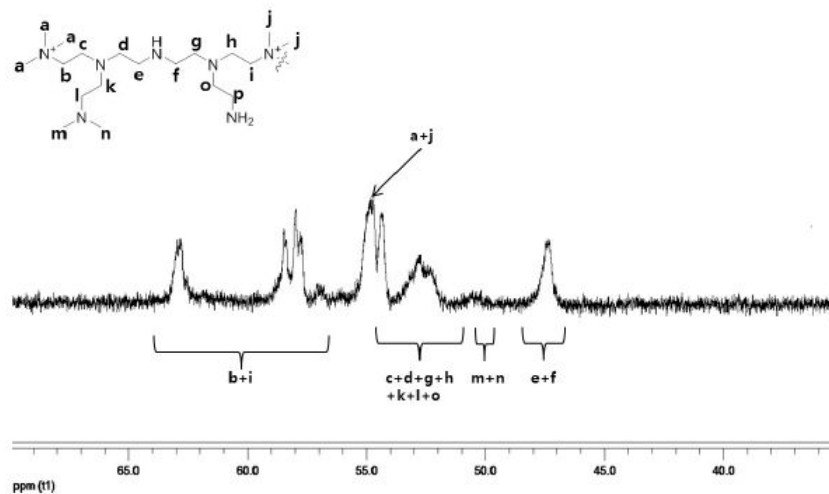


**Figure 5.** The inverted gate (INVGATE) <sup>13</sup>C NMR spectra of MPEII<sub>0.35</sub> (25 kDa) (A) and MPEII<sub>0.38</sub> (0.80 kDa) (B).

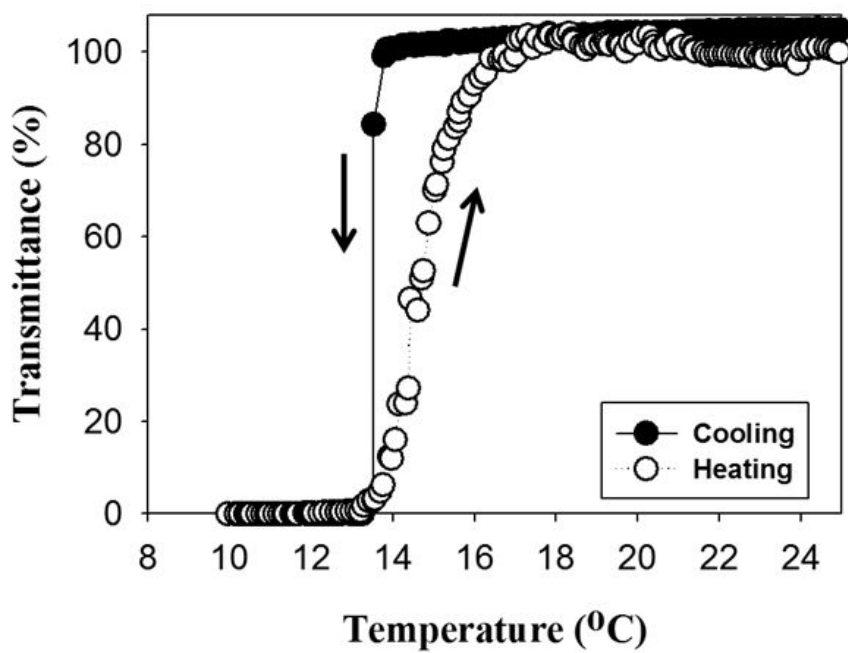


**Figure 6.** Hysteresis of MPEII<sub>0.35</sub> (25 kDa) at 20 % (w/w) polymer composition.

**Table 1.** pH values of (A) the PEI halide solutions and (B) MPEII solutions.

**A.**

	Composition (w/w%) <sup>b</sup>					
	HCl	HBr				HI
	20wt%	20wt%	25wt%	30wt%	35wt%	35wt%
1.5eq <sup>c</sup>	—	0.53	0.44	0.15	-0.25	0.25
2.0eq	—	0.40	0.33	0.050	—	—
2.5eq	—	0.20	-0.040	-0.22	—	—
4.0eq	-0.40	—	—	—	—	—

**B.**

	Composition (w/w%) <sup>b</sup>					
	10wt%	20wt%	30wt%	35wt%	40wt%	50wt%
MPEII <sub>0.38</sub> (0.80 kDa)	3.7	3.4	3.4	—	3.4	3.6
MPEII <sub>0.35</sub> (25 kDa)	4.4	4.4	—	4.6	—	4.3

<sup>a</sup> The pH value of the solution was measured by the pH meter (SevenEasy™, Mettler-Toledo, Switzerland) with the appropriate pH range of 2–11. Extreme pH values were automatically calculated by the instrument through extrapolation.

<sup>b</sup> Composition of polymer halide salts in water.

<sup>c</sup> Equivalent of HX to total amines (N) in *b*-PEI.



## List of publications

1. Heejin Kim, Seonju Lee, Minwoo Noh, So Hyun Lee, Yeongbong Mok, Geun-woo Jin, Ji-Hun Seo, Yan Lee, Thermosensitivity Control of Polyethylenimine by Simple Acylation, *Polymer*, 52(6), 1367–1374 (2011)
2. Minwoo Noh, Yeongbong Mok, Seonju Lee, Heejin Kim, So Hyun Lee, Geun-woo Jin, Ji-Hun Seo, Heebeom Koo, Tae Ha Park, Yan Lee, Novel Lower Critical Solution Temperature Phase Transition Materials Effectively Control Osmosis by Mild Temperature Changes, *Chemical Communications*, 48(32), 3845–3847 (2012)
3. Sangmok Jang, Seonju Lee, Heejin Kim, Jiyeon Ham, Ji-Hun Seo, Yeongbong Mok, Minwoo Noh, Yan Lee, Preparation of pH-sensitive CaP Nanoparticles Coated with a Phosphate-based Block Copolymer for Efficient Gene Delivery, *Polymer*, 53(21), 4678–4685 (2012)
4. Minwoo Noh, Yeongbong Mok, Daichi Nakayama, Sangmok Jang, Seonju Lee, Taeho Kim, Yan Lee, Introduction of pH-Sensitive Upper Critical Solution Temperature (UCST) Properties into Branched Polyethylenimine, *Polymer*, 54(20), 5338–5344 (2013)

5. Yeongbong Mok, Daichi Nakayama, Minwoo Noh, Sangmok Jang, Taeho Kim, Yan Lee, Circulatory Osmotic Desalination Driven by a Mild Temperature Gradient Based on Lower Critical Solution Temperature (LCST) Phase Transition Materials, *Physical Chemistry Chemical Physics*, 15(44), 19510–19517 (2013)
  
6. Daichi Nakayama, Yeongbong Mok, Minwoo Noh, Jeongseon Park, Sunyoung Kang, Yan Lee, Lower Critical Solution Temperature (LCST) Phase Separation of Glycol Ethers for Forward Osmotic Control, *Physical Chemistry Chemical Physics*, 16(11), 5319–5325 (2014)
  
7. Minwoo Noh, Sunah Kang, Yeongbong Mok, So Jung Choi, Jeongseon Park, Jannick Kingma, Ji-Hun Seo, Yan Lee, Upper critical solution temperature (UCST) phase transition of halide salts of branched polyethylenimine and methylated branched polyethylenimine in aqueous solutions, *Chemical Communications*, accepted

## Abstract in Korean (국문초록)

“스마트재료”(Smart materials)란 물리적인 신호인 온도, 빛, 자기장 뿐만 아니라 화학적 신호인 이온 농도, 글루타티온 농도, pH 등의 외부 신호에 반응하여 급격한 물리화학적 변화를 보이는 물질을 말한다. 특히 이중에서도 온도는 외부에서 쉽게 가해 줄 수 있으며 가역적인 변화를 일으킬 수 있다는 장점이 있다.

온도응답성 물질이라는 것은 2가지 이상의 물질을 섞을 때, 미세한 온도변화에 의하여 급격한 물리학적 또는 화학적 변화를 일으키는 것들을 말한다. 그 중에서도 나는 수용성 온도응답성물질에 주목을 하였다. 물은 지표면의 약 70%를 덮을 만큼 우리 주위에서 흔하게 볼 수 있을 뿐만 아니라 지구상 모든 생물체의 체액을 이루는 주 물질이기 때문에 수용성 온도응답성은 생체의학/생화학 분야 뿐만 아니라 수처리 분야에도 광범위하게 응용될 수 있다. 실제로 이러한 수용성 온도응답성 물질의 특성을 이용하여 세포배양접시, 크로마토그래피, 온도촉진약물전달, 표적약물전달 등의 다양한 분야에 응용하고 있다.

수용성 온도응답성 물질은 흔히 2가지로 분류 할 수 있으며 수용액 내에서 온도응답성 물질의 상전이는 다음의 간단한 열역학식에 의하여 설명을 할 수 있다.

$$\Delta G_m = \Delta H_m - T\Delta S_m$$

(혼합의 깁스자유에너지:  $\Delta G_m$ , 혼합의 엔탈피:  $\Delta H_m$ , 혼합의 엔트로피:  $\Delta S_m$ , 온도; T)

어떤 온도 이하에서는 물에 대한 좋은 용해도를 보이다가 그 온도 이상에서는 물에 대한 용해도가 급격히 떨어져 석출되는 물질을 저임계용해온도 물질(Lower critical solution temperature; LCST)이라고 한다. LCST의 대표적인 물질은 폴리아이소프로필아크릴아마이드이며 이 물질은 친수성 부분과 소수성 부분이 적절히 균형을 이루고 있다. 수용액 내에서 이러한 고분자는 물에 대한 용해도가 좋아 혼합의 엔탈피( $\Delta H_m$ )가 음수 값을 갖게 되며, 물 분자들이 무질서한 형태로 존재하다가 고분자의 소수성 부분을 정돈 된 형태의 격자모양으로 수화시켜야 하기 때문에 혼합의 엔트로피( $\Delta S_m$ )가 큰 음의 값을 갖게 된다. 따라서 위의 식에 따르면 온도가 높아지게

되면 온도와 혼합의 엔트로피의 곱이 음수 값의 혼합의 엔탈피 ( $\Delta H_m$ ) 보다 같거나 커져 혼합의 깃스자유에너지( $\Delta G_m$ )가 0이상이 되어 상전이가 일어나게 된다.

어떤 온도 이상에서는 물에 대한 좋은 용해도를 보이다가 그 온도 이하에서는 물에 대한 용해도가 급격히 떨어져 석출되는 물질을 고임계용해온도 물질(Upper critical solution temperature)이라고 한다. 이러한 UCST특성을 보이는 물질은 분자 내 또는 분자간의 결합을 강하게 할 수 있는 작용기를 많이 가지고 있다는 것이 특징이다. 예를 들어, 폴리-3-다이메틸(메타아크릴로일옥시에틸) 암모늄 프로페인 술포네이트는 양전하와 음전하를 동시에 갖고 있어 분자 내 또는 분자 간의 강한 결합을 하기 때문에 혼합의 엔탈피가( $\Delta H_m$ ) 양의 값을 갖게 된다. 따라서 이 분자는 온도가 높았을 때는 양의 값을 갖고 있는 혼합의 엔트로피( $\Delta S_m$ )와 온도의 곱이 혼합의 엔탈피( $\Delta H_m$ ) 보다 작아서 물에 잘 녹아 있다가 온도가 낮을 때는 혼합의 깃스자유에너지( $\Delta G_m$ )가 양의 값을 갖게 되어 상전이가 일어나게 된다.

나는 위에서 언급한 수용액 내에서 온도응답성을 갖는 물질을 기존의 방법보다 간편하게 만드는 방법을 이 학위논문에서 제안을 하고자 한다. 기존의 방법들은 단량체를 합성하고 이 단량체를 중합하여 고분자를 만들어야 한다는 어려움이 있었다. 그래서 나는 기존의 방법과는 다르게 상업적으로 구입 가능한 가지형 폴리에틸렌이민을 구입하여 아실레이션, 고리 열림반응, 메틸화 반응 등 간단한 반응을 통하여 LCST물질 뿐만 아니라 UCST물질을 합성하였다. 또한 바이오메디컬분야에 집중되어 있는 응용분야에서 벗어나 온도응답성 물질을 정삼투유도용질로 이용한 새로운 응용분야를 제안하였다.

폴리에틸렌이민은 반응성이 좋은 다량의 아민기를 가지고 있기 때문에 간단한 아실레이션을 통하여 폴리아이소프로필아크릴아마이드와 유사한 LCST물질을 합성할 수 있었고 이렇게 합성된 아실화 폴리에틸렌이민은 치환체의 소수성기, 아실레이션 정도, pH 등의 변화를 통해 10-90 °C의 원하는 상전이 온도를 조절할 수 있었다.

이에 더하여 가지형 폴리에틸렌이민을 사용하여 1,3-프로페인 술포네이트의 고리열림 반응을 통하여 폴리-3-다이메틸(메타아크릴로일옥시에틸) 암모늄 프로페인 술포네이트와 유사한 구조를 갖는 UCST물질을 합성하였다. 술

포프로필화 폴리에틸렌이민 유도체들은 수용액 내에서 분자 내에 양전하와 음전하를 모두 가질 수 있기 때문에 강한 분자간 결합(>0) 을 통하여 UCST현상을 갖으며 고분자의 분자량, 술포프로필화의 치환 정도, pH, 이온 농도 등의 변화를 통하여 10-90 °C 범위 내에서 상전이 온도를 조절할 수 있었다.

수용액 내에서 양이온과 음이온이 떨어져 있다고 하더라도 강한 상호작용을 할 수 있는 시스템을 만든다면 이온성 염의 형태로도 고임계용해온도 현상 물질을 만들 수 있을 것이라고 생각을 하였다. 가지형 폴리에틸렌이민과 할로겐화수소를 섞어 폴리에틸렌이미늄할로겐염을 만들거나 아이오도메테인을 섞어 메틸화된 폴리에틸렌이민을 합성하였다. 폴리에틸렌이미늄 할로겐염은 UCST상전이현상을 보이지만 산성도가 너무 낮아 실용적인 응용에는 제한이 있었다. 그러나 메틸화된 폴리에틸렌이민은 35-38% 정도의 영구적인 양전하를 갖는 4차 암모늄을 갖고 있고 이에 상응하는 양의 I<sup>-</sup> (쪽이온)을 갖게 되면 양전하와 음전하의 정전기적인력 뿐만 아니라 소수성 상호작용으로 인하여 적당한 산성도에서 고임계용해온도 현상을 보였다. 같은 이유로 요오드 이온을 보다 더 소수성을 갖는 이온 테트라플루오르보레이트로 치환을 했을 경우에는 더 높은 온도에서 상전이 온도를 보였다. 하지만 상대적으로 친수성 이온인 염소이온, 브롬이온으로 치환했을 때는 상전이 온도를 보이질 않았다. 또한 다양한 염의 비율 뿐만 아니라 이온 세기의 변화, 분자량 등의 변화가 메틸화된 폴리에틸렌이민의 상전이 온도에 미치는 영향을 연구하였다.

온도응답성을 아민을 다량 포함하고 있는 고분자에 쉽게 도입할 수 있는 기술을 개발하였기 때문에 기존의 바이오메디컬응용 분야에 국한되어 있던 응용분야에서 벗어나 정삼투공정의 유도용질로의 새로운 응용이 가능할 것이라고 생각한다. 정삼투법은 반투막을 사이에 두고 한쪽에는 거르고자 하는 입자를 포함하고 있는 피드용액을 넣고 다른 한쪽은 피드용액보다 높은 농도의 유도용질을 녹여 삼투압차이를 이용하여 자연적인 삼투현상으로 청수를 얻는 방법이다. 반트-호프 방정식에 의하면 삼투압은 분자량에 반비례하기 때문에 단분자이면서 높은 수용해도를 갖는 물질이 필요하였다.

$$\pi = c.R.T = w/(V.M).R.T$$

(c: 몰농도, R: 기체상수, T: 온도, V: 용액의 부피, M: 용질의 분자량, w: 용질의 무게)

따라서 나는 LCST물질인 nBu-PEI의 구조로부터 영감을 받아 단분자인 nBu-TAEA(356g/mol)을 합성하였고 이의 LCST현상을 확인하였다. nBu-TAEA는 2.2 M이라는 높은 수용해도를 보이면서도 20-30 °C라는 상온 수준의 상전이 온도를 보였기 때문에 적은 에너지의 사용으로 용질의 제거가 가능하였다. 상전이 온도보다 낮은 온도에서는 반투막을 사이에 두고 해수 (0.60M)로부터 청수를 얻을 수 있었고 상전이 온도 이상의 온도에서는 물에 대한 용해도가 급격히 떨어져 0.15M보다 작은 농도가 되어 생리식염수 수준(0.15M)의 염수로 청수를 내 보낼 수 있었다. 이러한 온도응답성 물질을 유도용질로 사용한 정삼투 공정은 미래의 에너지효율적인 수자원 확보를 위한 좋은 예가 될 수 있을 것 이라고 기대한다.

#### Keywords

온도응답성물질, 저임계용해온도(LCST), 고임계용해온도(UCST), 정삼투(FO), 가지형폴리에틸렌이민

Student number : 2010-20275